The Diabatic and Nonlinear Aspects of the El Nino-Southern Oscillation: Implications for its Past and Future Behavior

De-Zheng Sun

University of Colorado/Cooperative Institute for Research in Environmental Sciences &NOAA Earth System Research Laboratory/Physical Science Division, Boulder, Colorado, USA
http://www.cdc.noaa.gov/people/dezheng.sun/

March 20, 2009

Submitted to

AGU Monograph "Climate Dynamics: Why Does Climate Vary?"

Revised

November 20, 2009

Abstract

This chapter reviews recent advances in understanding the diabatic and nonlinear aspects of ENSO. In particular, it reviews the research leading to the view that averaged over the decadal or longer time scales, ENSO acts as a basin-scale heat mixer in the tropical Pacific. This heat mixer regulates the long-term temperature difference between the surface water in the warm-pool and the subsurface water constituting the equatorial undercurrent. When this temperature difference is externally forced to increase, the level of ENSO activity increases. Conversely, when this temperature difference is externally forced to decrease, the level of ENSO activity decreases. The time-mean effect of ENSO is to counteract the effect of external forcing on this temperature difference.

This view of ENSO explains the recent trend in the level of ENSO activity in the instrumental record and sheds light on the behavior of ENSO in the past climates. The implied response in the level of ENSO activity to global warming, however, is at odds with the popular prediction by the state-of-the-art coupled climate models. Reasons for this discrepancy are explored. An inadequate sensitivity of the tropical hydrological cycle to SST changes in the present coupled models is hypothesized as a possible factor responsible for the discrepancy.

1. Introduction

The steady increase in the CO2 concentration and other man-made greenhouse gases in the atmosphere has caused due concern about the future of the state of the Earth's climate system (IPCC 2007). A question of prominence is what is the impact of the enhanced radiative heating in the atmosphere on the amplitude of natural variability in the climate system, in particular, those natural modes that have a global reach in causing climate anomalies (Trenberth et al. 1998; Glantz 2001 McPhaden et al. 2006). On this radar screen, ENSO figures prominently. ENSO not only causes anomalies in the seasonal mean temperature and precipitation world-wide (Ropelewski and Halpert 1996, Hoerling and Kumar 2003, Huang and Wu 1989, Wang et al. 2008, Penland et al., this volume), it also affects the statistics of the extreme weather events, such as hurricanes/typhoons (O'Brien and Richards 1996) and mid latitude severe storms (Barsugli et al. 1999, Cayan et al. 2000, Meehl et al. 2005). Arguably, how the enhanced radiative heating due to the increasing CO2 concentration in the atmosphere influences ENSO is one of the most important questions in the science of global climate change.

The most sophisticated tools to address this question are the state-of-the-art of the coupled models, but the biases in the simulated tropical Pacific climate by these models undermine the confidence in the results from these models (Sun et al. 2006, Lin 2007, Guilyardi et al. 2009, Sun et al. 2009). The complexity of these models also hinders understanding. The original theoretical framework developed to explain ENSO as a climate anomaly growing and decaying about a prescribed mean climate state (Zebiak and Cane 1988 and others), has shed important light onto this question (Clement et al. 1996, Cane et al. 1999). Because the Z-C model is an anomaly model and does not have an explicit heat budget for the subsurface ocean, the response of this model to an increase in the radiative heating is subject to question (Cane 2004). The Z-C model also left the feedback from ENSO onto the mean climate unaddressed.

This chapter attempts to provide a more systematic examination of the relationship of ENSO with radiative heating over the Pacific Ocean, assess and delineate the collective effects of ENSO on the mean state. Because of the length restriction, the material reviewed will be focused on the research by the author and his collaborators. The goal is to present an extended picture of ENSO that not only reaffirms the importance of the dynamics coupling—the Bjerknes feedback-- in giving rise to this important phenomenon (see review by Neelin et al. 1998), but also highlights a fundamental force that set the

background stage for this positive feedback to operate---the meridional differential heating over the Pacific ocean. This force destabilizes the coupled tropical ocean-atmosphere through its impact on the temperature difference between the warmpool SST (Tw) and the equatorial thermocline water (Tc) (Sun 2003, Sun et al. 2004). More importantly, it will be shown that by repeatedly sloshing the tropical upper ocean water, ENSO acts as basin-scale heat mixer that regulates the long-term mean value of this temperature contrast (Sun and Zhang 2006, Sun 2007).

This extended picture of ENSO suggests an interesting scenario for the response of ENSO to global warming. During the initial stage of global warming, Tw-Tc is likely to increase due to the forcing from global warming. An elevated ENSO activity then ensues in response. During the late stage of global warming, however, Tw-Tc is likely to decrease in response to the flux of warmer extratropical surface water to the subsurface of the equatorial Pacific. Then the level of ENSO activity may reduce. Do observational data support this scenario? Do the results from the state-of-the-art models support this scenario? If not, why? This chapter also attempts to provide some discussion about these questions that may be useful for further research.

This chapter is organized as follows. We first review the theoretical progress that has been made on the diabatic and nonlinear aspects of ENSO. We then present an analysis of the recent elevation of ENSO activity as a first test of the theory developed. We then review paleo-climate findings concerning the behavior of ENSO in the past climates and examine whether the past behavior of ENSO can be explained by the theoretical results. Finally, we discuss the simulations by IPCC models of the response of ENSO to global warming, and explain the discrepancies between the model simulations/projections and the theoretical predictions

2. Theoretical advances:

2.1 Insights from an analytical model

An analytical model was first used by the author to address the question of the impact of global warming on ENSO (Sun 1997, 2000). The coupled tropical Pacific ocean-atmosphere system is represented by a few boxes—one box for the atmosphere, two boxes for the surfaces oceans—the western and eastern surface Pacific--and one box for the subsurface upper ocean (Fig. 1a). The thermodynamical effect of the atmosphere is to heat the ocean to a zonally uniform SST (Tw) if not opposed by ocean transport (See Eqs.

(6) and (7) in Sun 2000). (Tw has been called the radiative convective equilibrium SST and may be regarded as the tropical maxiumum SST or the SST of the warmpool). The zonal wind stress is coupled to the zonal SST contrast (Eq. (8) in Sun 2000). The treatment of upper ocean dynamics is based on the recharge and discharge oscillator model of Jin (1996), but with zonal advection added (see Eqs. 11, 12, 13,14 in Sun 2000). The reference temperature profile for the subsurface box is further assumed to be determined by a balance between the surface heating from above and the cooling from upwelling of cold water from below. With realistic parameters, the model simulates the essential aspects of ENSO including the preferred period, the westward propagation of the SST anomalies, and the phase relationship between SST and the depth of the thermocline in the eastern Pacific (Fig. 1bc). The oscillation is not always regular in the model, depending on the strength of the zonal advection relative to the strength of the total upwelling, as noted by Timmermann and Jin (2001). Whether ENSO may be more adequately described as series of events or as a cycle was discussed by Kessler (2002). The asymmetry of ENSO in this model depends on the reference temperature profile for the thermocline (Eq. (10) in Sun 2000).

The advantage of using an analytical model is that the behavior of the model in the full range of its parameter space can be easily obtained. An exploration of the behavior in the

full range of its parameter space reveals that the system does not have to oscillate. It does not even have to have substantial zonal SST contrast as we have observed today. The reason that we have zonal SST contrast and an oscillatory behavior is because the warm-pool SST is sufficiently high relative to the temperature of the equatorial undercurrent. These insights are drawn from Fig 2a which shows the equilibrium change of the area mean SST of the eastern and western Pacific as a function of Tw (or Tw-Tc as Tc is kept fixed). The figure shows that when the value of Tw is sufficiently low, there is no zonal SST contrast. As the value of Tw becomes progressively high, the system experiences a picth-fork bifurcation to create the zonal SST contrast, then a Hopf bifurcation to enter an oscillatory state. Once the system enters the oscillatory state, the amplitude of oscillation increases with further increases in Tw (Fig .2b).

Critical for the instability of the steady circulation—the onset of an oscillatory regime-- is that the temperature of the upwelled water depends strongly on the strength of the flow rate and that the flow rate (or the thermal forcing that drives the flow) is sufficiently large relative to the thermal and mechanical damping (Sun 1997). An analogous mechanism is responsible for the onset of oscillation in the Lorenz system (Lorenz1 963) which is a low-order approximation of Rayleigh-Benard convection. Indeed, the oscillation in the present model does not have to be periodic—it can be chaotic (Timmermann and Jin

2001). Thus, the present explanation for the existence of ENSO may be regarded more fundamental than the traditional explanation attributing the "turn around" or the phase change of the ENSO to a delayed feedback from the subsurface ocean.

2.2. An implied role for the extratropics

Further recognizing the water feeding the equatorial thermocline comes from the extratropics (Pedlosky 1987, McCreary and Lu 1994, Liu et al. 1994), we further expanded the model to illustrate a possible role of extratropical warming/cooling from the high latitudes (Fig. 3a). In this model, the temperature of the equatorial undercurrent (T_c) IS directly linked to the extratropical SST (T_3). The equations governing the equatorial SST and the depth of the equatorial thermocline are the same as those for the model shown in Fig. 1a. Fig.3b shows the mean SST as a function of the extratropical Pacific SST (T_3). (The dashed lines are for the equilibrium SST that become unstable). The figure shows that when the value of T_3 is sufficiently high relative to the value of Tw, there is no zonal SST contrast. As the value of T_3 becomes progressively low, the system experiences a picth-fork bifurcation to create the zonal SST contrast, then a Hopf bifurcation to enter an oscillatory state. Once the system enters the oscillatory state, the amplitude of oscillation increases with further decreases in T_3 (Fig.3c). Thus, it appears

that the extratropical cooling has the same impact as that from the tropical heating on the zonal SST contrast and the amplitude of ENSO.

2.3 Results from a numerical model

We then replaced the box model by NCAR's Pacific basin model—the primitive equation model of Gent and Cane (1989). Details of the hybrid coupled model are provided in Sun (2003) and Sun et al. (2004). The results from this more complicated model confirm the results from the analytical model (Fig. 4ab): either an increase in the tropical heating or an increase in the extratropical cooling may increase the amplitude of ENSO. Note that the impact from the extratropical cooling on the level of ENSO activity is not immediate, but with a delay (Fig. 4b). This is because it takes time for the cold surface water of the extratropical ocean to reach the equatorial subsurface via the subduction process (Pedlosky 1987, McCeary and Lu 1994, Sun et al. 2004). As in the box model, annual cycle is not included in this hybrid model.

2.4. Feedback from ENSO onto the mean state

The results from the hybrid model also reveals that ENSO changes may feedback onto the mean climate state (i.e., its background state), in particular, onto the difference between the warm-pool SST (Tw) and the temperature of the equatorial undercurrent (Tc). Table I lists results from three pairs of experiments designed to contrast the response of Tw, Tc, and Tw-Tc, in response to an enhanced tropical heating between the case with ENSO and the case without ENSO. (The case without ENSO refers to a case in which the equatorial ocean-atmosphere is not dynamically coupled: the winds are constant). In all three pairs, the response in Tw-Tc to tropical heating is much reduced in the case of ENSO than in the case without ENSO.

Fig.5a and Fig.5b provide a more detailed look of the response in the time-mean temperature of the equatorial upper ocean. These two figures show respectively the equatorial temperature differences (5^oS--5^oN) between the control run and the perturbed run for the case without ENSO (Fig.5a) and for the case with ENSO (Fig. 5b). Without ENSO, the warming of the tropical ocean is essentially confined to the surface layer with the response in the western Pacific being slightly deeper than in the eastern Pacific. With ENSO, the response extends to the themocline. While the thermocline water is much warmer in the case with ENSO, the response at the surface western Pacific is reduced.

This feedback of ENSO as evident in Fig. 5 is linked to the asymmetric response in the two phases of ENSO. Stronger La Nina is accompanied with stringer winds which enables more heat to be pumped downward to the subsurface ocean--the western Part of the ocean in particular in the equatorial region. Fig. 6a shows the upper ocean temperature changes during La Nina events in response to the enhanced tropical heating. The thermocline is deeper in the western Pacific consistent with the stronger zonal winds. Fig.6b shows the temperature differences in the warm-phase. Stronger El Nino events then warm the upper ocean in the central and eastern Pacific. Averaged over the cold and warm phases, the heat is "mixed" downward across the basin.

The feedback of ENSO onto the mean climate also shows up in the extratropical cooling experiments. A typical response in the time-mean temperature of the equatorial upper ocean (5^oS--5^oN) to an enhanced extratropical cooling is shown in Fig.7a for the case without ENSO and in Fig.7b for the case with ENSO. Without ENSO, the equatorial thermocline water (Tc) is cooled by about 1^oC by the imposed cooling over the subtropical surface ocean. The cooling of the equatorial ocean is largely confined to the subsurface--the cooling of the western Pacific SST (Tw) is negligible. With ENSO, the cooling of the thermocline water is reduced down to about 0.5^oC while the cooling of the surface western Pacific is enhanced by about the same amount.

Fig. 8 further shows a meridional section of the ocean temperature change at the central Pacific. Again, the left is the case without ENSO, and the right panel is for the case with ENSO. The role of subduction in carrying the cooling from the extratropics to the equatorial subsurface is evident in the case without ENSO. With ENSO, the equatorial region and the high latitudes appear to be disconnected, particularly in the north hemisphere. This may provide an explanation for why it is difficult to trace decadal temperature anomaly in the real world all the way from the extratropics to the equatorial Pacific (Deser et al. 1996, Schneider et al. 1999). The real world has recurrent occurrence of ENSO events which effectively destroys the temperature anomalies on the decadal and longer time scales though effective mixing in the tropical Pacific. Therefore the apparent disappearance of decadal temperature anomalies upon their reach to the equatorial region in the observations does NOT suggest an ineffective extratropical influence over the level of ENSO activity.

This feedback of ENSO as evident in the cooling case again is linked to the asymmetric response in the two phases of ENSO. Fig. 9 shows respectively the upper ocean temperature changes during La Nina events and the El Nino events. The cooling to the western Pacific occurs only in the warm phase, and the cooling to the eastern Pacific

occurs only in the cold phase. Despite the imposed extratropical cooling, the eastern Pacific actually becomes warmer in the warm phase. Warming also occurs in the western Pacific during the cold phase.

The reduced sensitivity in Tw-Tc to external forcing in the presence of ENSO underscore the fact that ENSO has a time-mean effect on the mean state. To further investigate the effects of ENSO on the mean climate, a pair of forced experiments are conducted. In one of them, the climatolgical surface wind stress over 1950—1999 is used while in the other, the surface wind stress is climatological winds plus the interannual monthly anomalies (i.e., the actual monthly surface wind stress for the period 1950-1999). The long-term means of the surface wind stress in the two runs are thus identical. The two experiments also use the same restoring boundary conditions---the SST is restored to the same prescribed SST. The resulting equilibrium upper ocean temperatures are respectively shown in Fig. 10a and Fig. 10b. The case with fluctuating surface wind stress has a shallower warm-pool, but a thicker and more diffused thermocline. This effect of the fluctuating wind (the presence of ENSO) is more evidently shown in Fig. 11a which shows the difference in the equilibrium upper ocean temperature between these two phases. The figure shows again that the role of ENSO is to cool the western Pacific warm pool, but warm the subsurface thermocline water. We have also found that with the

fluctuating part of the wind stress being magnified by 50%, the effect of ENSO on the mean upper ocean temperature is increased proportionally (Fig. 11b). The exact mechanism for such a rectification effect is being investigated. Preliminary results suggest that the nonlinear "eddy" heating (i.e., the convergence of $\overline{V'T'}$—where V' and T' are respectively the fluctuating part of the velocity and temperature owing to ENSO, and the over-bar denotes the time-average over many cycles of ENSO) is a primary source for this effect. Note that here the "eddy" refers to part of the fluctuating part of the motion.

2.5 A null hypothesis for the response of ENSO to global warming

The theoretical analysis suggests that collectively, ENSO events act as a basin-scale heat exchanger that regulates the climatological temperature contrast between the warmpool (Tw) and the thermocline water (Tc). The level of ENSO activity may be proportion to the externally forced tendency in Tw-Tc. Global warming is likely to force Tw-Tc to increase first because the surface feels the warming first. Eventually, however, because of the connection between the surface water over the extratropical Pacific and the subsurface water of the equatorial Pacific, the temperature of the subsurface water of the equatorial Pacific may increase at a rate more than the increase in the warmpool SST.

Thus, the following scenario about how ENSO responds to global warming is raised: Global Warming would initially force an elevated ENSO activity--a more vigorous sloshing of the upper ocean water in the tropical Pacific. But the end result is likely the "death" of ENSO (or put it more sanguinely, the creation of a permanent El Nino—a permanently warm state in the equatorial eastern Pacific). This scenario may serve as a useful null hypothesis in understanding the response of ENSO to global warming.

3. Recent Elevation of ENSO Activity

The recent elevation of ENSO activity over the last few decades offers a test of the relevance of the aforementioned theoretical results. Nino3 SST anomalies in the instrumental record, together with its variance calculated using a moving window with a width of 16 years, are shown in Fig. 12. The level of ENSO activity, measured by the variance on the decadal time-scale, exhibits an upward trend over the last century. The trend is particularly impressive in the most recent three decades. The elevation of ENSO activity over the last 30 years is also evident in the variability in the subsurface temperature of the equatorial Pacific. Fig. 13a shows respectively the subsurface temperature anomalies in the eastern and western Pacific, and Fig. 13b is the difference between the two. ENSO involves a zonal redistribution of equatorial upper ocean water,

causing warming in the eastern upper ocean and cooling in subsurface of the western Pacific. Thus the difference between the subsurface temperature in these two regions is arguably a more complete measure of the ENSO activity.

Is this elevation consistent with the theory developed in the previous sections? The upper panel of Fig. 14 shows the time series of tropical maximum SST (which may be regarded as the Tw in the analytical model) that corresponds to the Nino3 SST time series in Fig. 12. Overall, the trend over the last century is positive, but the rate of increase over the past three decades or so is particularly impressive. This rapid increase in the value of Tw corresponds to the elevated ENSO activity as shown in Fig. 12. The lower panel shows the global distribution of SST trend over the last three decades. Note that while the warmpool SST has been increasing, the corresponding trend in the eastern equatorial Pacific is negative. So the last 30 years corresponds to a period with a strengthening zonal SST contrast. Consistent with the negative trend in the eastern equatorial Pacific, the subsurface of the equatorial eastern Pacific, and the connected thermocline water temperature (Tc) also have a negative trend (Fig. 15). Clearly, the difference between the warmpool SST and the temperature of the equatorial thermocline water (Tw-Tc) over the last three decades or so has been increasing. So the relationship between the tendency

in Tw and Tc and the anomalous activity of ENSO in this period is consistent with the theoretical prediction.

Will the elevated ENSO activity likely to continue? Fig. 16 shows the time series of Tw-Tc. As indicated by this stability measure, the coupled system is clearly less stable than the previous decades. There is not yet a clear hint from this time series that this elevation in Tw-Tc is beginning to wane. So we expect the anomalous activity of ENSO is likely to continue into the coming decades.

4. ENSO in the past climates

Proxy data about the behavior of the past climates offers more opportunities to test the relevance of our theoretical results. One finding concerning the behavior of ENSO in the past climates is that it has a long history—a continuing presence up to 3 millions ear ago (Fedorov et al. 2006). The collateral question is why it did not exist before then. An examination of the evolution of the zonal SST contrast indicates that the birth of ENSO corresponds to a time when the zonal SST contrast reaches a substantial value (Fig. 17) (Wara et al. 2005). Fig. 17 shows the proxy SST records for the tropics Pacific over the last 5 millions years. Before about 3 million year ago, the high latitudes were

considerably warmer (see Fig. 1 in Fedorov et al. 2006). This high latitude warmth may result in much warmer upwelling water in the equatorial zone, a much weakened zonal SST contrast (see Fig. 17), and consequently the disappearance of ENSO (or a permanent El Nino condition) (recall Fig. 3).

While ENSO is believed to have a 3 million year long continuing history, its level of activity has varied--at least in the last 1500 years (Moy et al. 2002, Cobb et al. 2003, Rein et al. 2004, Rein et al. 2005, Graham et al. 2007, Newton et al. 2006, Mann et al. 2009, Sachs et al. 2009). Of particular interest in the present context are those centennial-scale changes that correspond to the so-called Medieval Climate Anomaly (MCA) and the Little Ice Age (LIA)—periods during which distinct climate changes were also registered in the extratropical regions (Crowley and Lowery 2000, Bradley et al. 2003 Mann et al. 2009; Graham et al. 2007, Touet et al. 2009).

The proxy data by Rein et al. (2004) suggests a weak ENSO activity during the Medieval Warm Period (MWP) (Fig. 18). This finding is also supported by the inferred mean climate change during this period—which is La Nina-like (Pacific (Cobb et al. 2003, Graham et al. 2007, Conroy et al. 2008, Oppo et al. 2009, Mann et al. 2009). The relationship between the mean state change and the level of ENSO activity exhibited in

the instrumental record of the last 50 years is that a El Nino-like change in the mean state be accompanied by a higher level of ENSO activity and a La Nina change in the mean state be accompanied by a lower level of ENSO activity (Zhang et al. 1997, Vecchi et al. 2008). Such a relationship between the mean state and the level of ENSO activity is consistent with the observed asymmetry between the two phases of ENSO—El Nino on average is stronger than La Nina, so stronger ENSO activity translates into El Nino-like changes in the mean state (Zhang et al. 2009).

With regard to the LIA, the recent finding by Cobb et al. (2003) suggests that the level of ENSO activity during the Little Ice Age (LIA) is relative strong (Fig. 18). The inference for an elevated ENSO activity during the LIA is also consistent with the finding of a southward movement of the intertropical convergence zone (ITCZ) by Sachs et al. (2009).

In light of the theoretical analysis in the previous sections, it is tempting to hypothesize that the relatively strong ENSO during LIA and the relatively weak ENSO during MWP are again responses to changes in the Tw-Tc, which over the centennial time-scale, essentially the pole to equator temperature differences.

5. Possible problems with IPCC models.

The theoretical analysis and the paleo data suggest a sensitivity of ENSO to global climate change. State-of-the-art models, on the other hand, predict an almost muted response of ENSO to global warming. Early models with the use of flux adjustment predict a slight weakening of ENSO activity in response to global warming (Knutson et al. 1997, Meehl et al. 1993). More recent models without the use of flux adjustment suggest an even less sensitivity (Oldenborgh et al. 2006). The lack of sensitivity to global warming was also noted in a simulation of Eocene climate (Hueber and Calallero 2003).

How do we possibly reconcile the gap between the theoretical results and the GCM simulations of global warming? One possibility is that the models that the theoretical analysis is based on is too simple---we will return to this possibility in the last section of this chapter. The other possibility is that some relevant processes are still inadequately represented in the state-of-the-art climate models. Indeed, while there are general improvements in the AR4 models compared to their earlier versions (AnchutaRao and Spencer 2006), they still have errors in reproducing the observed ENSO events (Guilyardi et al. 2009). Particular relevance to the theoretical results in the present chapter is the asymmetry of ENSO, an aspect whose representation in the climate models

may be particularly problematic. The variance of Nino3 SST has been commonly used to measure the level of ENSO activity, but the asymmetry in the simulated ENSO may not correlate with the variance of Nino3 SST. Fig. 20a illustrate this point using the various version of NCAR CCSM as an example. The figure shows that while the variance of the Nino3 SST in the later versions of NCAR CCSM is comparable or even exceeds that from the observations, the skewness of the Nino3 SST is still far too weak (Fig. 20a). This is also true for the subsurface temperature of the equatorial eastern Pacific (Fig. 20b). The more symmetric ENSO in the models suggest that the processes that give rise to 'ENSO' in the models may be too linear.

The precipitation—SST relationship in the models are indeed too linear in the models than in the observations. Fig. 21a shows the relationship between precipitation and SST during ENSO over the equatorial Pacific in the observations and models. The figure shows that the observed SST and precipitation have a rather nonlinear relationship: the rate of increase of precipitation with SST picks up quickly once the SST exceeds its climatological value (i.e., near the zero point as is plotted here). The corresponding relationship in the models, in contrast, is more linear. Consequently, measured about their respective climatology, the precipitation increases with SST increases at a faster rate in the observations than that in the models. Only when the positive SST anomalies are very large, does the rate of increase of precipitation with respect to SST in some models

becomes more comparable to that in the observations. The corresponding figure for the surface level solar radiation shows that the relationship between the surface solar radiation and SST mirrors the relationship between precipitation and SST (Fig.21b). About its respective climatology, the surface solar radiation decreases at a faster rate in the observations than in the models. Clearly, measured either by the precipitation that deep convection produces, or by its reflectivity of solar radiation, deep convection in the observations responds more sensitively and more nonlinearly than in the models. Zhang et al. (2008) show that the improved ENSO asymmetry in the NCAR CCSM3.5 (Neale et al. 2008) is likely due to an improvement in the precipitation—SST relationship in the model. More studies are needed to address the full extent of the impact of a less responsive deep convection to SST increases on the response of the tropical climate to anthropogenic forcing. It is tempting to suspect, however, that an inadequately responsive deep convection in the models may be responsible for the lack of sensitivity of ENSO to global warming in the simulations by IPCC models.

6. Final Remarks:

Motivated to better understand the response of ENSO to global warming, we have attempted to address the following two issues: (1) what is the relationship between the

amplitude of ENSO and the radiative heating, (2) whether ENSO collectively constitutes an important feedback which in turn may determine the mean state. Our results suggest that the level of ENSO activity (on decadal and longer time scales) may be proportional to the tendency in the temperature difference between the surface water in the western Pacific warm-pool and the water constituting the equatorial undercurrent. Moreover, ENSO events may collectively act as a basin-scale heat mixer in the tropical Pacific that prevents the long-term mean value of the difference between the warm-pool SST and the temperature of the equatorial undercurrent from exceeding a critical value. The finding points to a mechanism by which global warming influences ENSO. Specifically, our finding raises the following scenario for the response of ENSO to global warming: An elevated level of ENSO activity is likely to occur during the initial stages of global warming, but a reduced level of ENSO activity (or even a permanent El Nino state) is likely to ensue when global warming is full-blown. The trend in the level of ENSO activity in the instrumental record appears to be consistent with this scenario. The behavior of ENSO in the past climates also supports this prediction. However, coupled GCM simulations fail to produce this scenario. It is suggested that an inadequate sensitivity of the tropical hydrological cycle in the models to SST changes due to a lack of strong nonlinearity in the deep convection—SST relationship may be responsible for the lack of response in the level of ENSO activity to global warming.

We would like to highlight some potential caveats in the theoretical results we have highlighted in this chapter. First, the results so far have been based on models that do not have the stochastic forcing from weather events. A significant role of stochastic forcing from weather events in the dynamics of ENSO has been suggested by a number of studies (Lau 1985, Kleeman and Power 1994, Penland and Sardeshmukh 1995, Chang et al. 1996, Wang et al. 1999, Kessler and Kleeman 2000). A particular illuminating result from these studies is that the irregularity in ENSO may be more easily explained as the presence of stochastic forcing than a consequence of chaotic dynamics. These studies, the linear inversed models of ENSO in particular, also suggest a role for the magnitude of the stochastic forcing from the weather events in determining the average magnitude ENSO. Thus, further studies need to include the stochastic aspects of the weather events. However, as the magnitude of the stochastic forcing from the weather events is likely dependent on the warm-pool SST, we expect that this additional forcing of ENSO should enhance the response of ENSO to global warming in the initial stage. Whether the enhanced weather forcing could outweigh the stabilizing effect from a reduced Tw-Tc in the later stage of global warming is clearly an enticing question for further investigation.

Another aspect that could complicate the proposed picture is the annual cycle—a factor

we have not been able to include in a realistic way in our theoretical models. ENSO is phase-locked to the annual cycle (Rasmusson and Carpenter 1982). While why this is so remains to be fully understood (Tziperman 1997, Cane 2004), the response of ENSO to global warming may depend on the response of the annual cycle to global warming. Indeed, Clement et al. (1996) interpreted the response of ENSO to a uniform increase in the radiative heating in the Z-C model in terms of the seasonal dependence of the growth rate of SST anomalies. An interesting feature of the Z-C model is that in response to a uniform increase in the restoring SST (equivalent to an increase in the tropical maximum SST as done in Sun 1997), the zonal SST contrast increases, but the level of ENSO activity does not (Clement et al. 1996, Cane et al. 2001) (Fig. 22). The latter result differs from that of Sun (1997). Sun (1997) suggested that the difference in the treatment of the subsurface temperature response to the increase in the surface heating could explain the difference in the response of ENSO amplitude. The subsequent studies of Sun (2003), Sun et al. (2004), and Sun and Zhang (2006) further underscore this possibility. However, the substantial variability in the level of ENSO activity on the decadal, centennial, and longer time-scale in the Z-C model also makes the inference of the response of an increase in the external heating a more involved issue. What is sure for now is that more studies are also needed to reconcile the results among simple models.

Acknowledgement

The work was supported by NOAA's Global Program and NSF's Large-Scale and Climate Dynamics Program and NSF's Physical Oceanography Program (ATM-9912434, ATM—0331760, and ATM 0553111). The author would thank Dr. Tao Zhang and Dr. Yongqiang Yu for their help in the research.

References:

AchutaRao K., and K. R. Sperber, 2006: ENSO simulation in coupled ocean-atmosphere models: are the current models better? *Climate Dynamics*, **27**, 1-15.

Barsugli J. J., J. S. Whitaker, A. F. Loughe, P. D. Sardeshmukh and Z. Toth, 1999: Effect of the 1997-98 El Niño on Individual Large-Scale Weather Events. Bull. Amer. Met. Soc., 80, pp. 1399-412.

Bradley R.S., M.K. Hughes, H. F. Diaz, 2003: Climate in Medieval Time. *Science,* **302**, 404-405.

Chen, C.C, B.A., McCarl, R.M., Adams, 2001: Economic implications of potential ENSO frequency and strength shifts, Climatic Change, 49, 147-159.

Cayan, D. R., K. T. Redmond, L. G. Riddle, 2000: ENSO and hydrological extremes in the western United states, J. Climate, 12, 2881-2893.

Cane, M., 2004: The evolution of El Nino, past and future. Earth and Planetary Science Letters, 164, 1-10.

Cane, M.A., A.C. Clement, A. Kaplan, Y. Kushnir, D. Poznyakov, R. Seager, S.E. Zebiak, and R. Murtugudde, 1997: Twentieth-century sea surface temperature trends, Science, 275, 957-960.

Carton, J.A., G. Chepurin**, X. Cao, and B.S. Giese, 2000a: A Simple Ocean Data Assimilation analysis of the global upper ocean 1950-1995, Part 1: methodology, J.Phys. Oceanogr., 30, 294-309.

Cess, R.D., and coauthors, 1990: Intercomparison and interpretation of climate feedback processes in 19 atmospheric general circulation models. J. Geophys. Res., 95, 16601-16615.

Chang, P., L. L. Ji, H. Li, and M. Flügel, 1996: Chaotic dynamics versus stochastic processes in El Nino-Southern Oscillation in coupled ocean-atmosphere models. Physica D, 98, 301-320.

Clement, A., and R. Seager, 1999: Climate and Tropical oceans. J. Climate, 12, 3383-3401

Clement, A., R. Seager, and M. A. Cane, 2000: Suppression of El Nino during the mid-Holocence by changes in the earth's orbit. Paleoceanography, 15, 731-737.

Clement, A., R. Seager, M. A. Cane, S. E. Zebiak, 1996: An ocean dynamical thermostat. J. Climate, 9, 2190-2196.

Cobb, K.M, C.D. Charles, H. Cheng, and R.L. Edwards, 2003: Coral records of the El Niño-Southern Oscillation and tropical pacific climate over the last millennium. Nature, 424, 271—276.

Collins, M., 2001: Understanding uncertainties in the response of ENSO to greenhouse

warming. Geophys. Res. Lett., 27, 3509-3512.

Collins, W. D., P. J. Rasch, B. A. Boville, J. J. Hack, J. R. McCaa, D. L. Williamson, J. T. Kiehl, B. Briegleb, C. Bitz, S.-J. Lin, M. Zhang, and Y. Dai, 2004: Description of the NCAR Community Atmosphere Model (CAM 3.0), Technical Report NCAR/TN-464+STR, National Center for Atmospheric Research, Boulder, Colorado, 210 pp.

Conroy, J. L., A. Restrepo, J. T. Overpeck, M. Steinitz-Kannan, J. E. Cole, M. B. Bush and P. A. Colinvaux, 2008: Unprecedented recent warming of surface temperatures in the eastern tropical Pacific Ocean, *Nature*, doi:10.1038/ngeo390.

Crowley, T.J., and T.S. Lowery, 2000: How Warm Was the Medieval Warm Period? *AMBIO*, **29**, 51-54.

Deser, C., M. A. Alexander, and M. Timlin, 1996: Upper ocean thermal variations in the North Pacific during 1970–1991. Journal of Climate, 9, 1840–1855.

Deser, Clara, Antonietta Capotondi, R. Saravanan, and Adam S. Phillips, 2005: Tropical Pacific and Atlantic Climate Variability in CCSM3. Journal of Climate (CCSM3 Special Issue): submitted.

Fedorov A.V., and S. G. Philander, 2000: Is El Nino Changing? Science, 288, 1997-2002.

Fedorov, A.V, and S.G. Philander, 2001: A Stability Analysis of Tropical Ocean-Atmosphere Interactions: Bridging Measurements and Theory for El Nino. J. Climate, 2001, 3086-3101

Fedorov, A., and S.G. Philander, 2001: A Stability Analysis of Tropical Ocean-Atmosphere Interactions: Bridging Measurements and Theory for El Nino. J. Climate, 14, 3086-3101.

Fedorov, A, P S Dekens, M McCarthy, A C Ravelo, P B deMenocal, M Barreiro, Ronald C Pacanowski, and S.G.H. Philander, 2006: The Pliocene Paradox (Mechanisms for a Permanent El Niño). 312(5779), 1485-1489.

Glantz, M.H., 2001: Currents of Change: Impacts of El Niño and La Niña on Climate and Society. Cambridge University Press, 252 pp.

Graham, N.E., M.K. Hughes, C.M. Ammann, K.M. Cobb, M.P. Hoerling, D.J. Kennett, J. P. Kennett, B. Rein, Lowell. Stott, P.E. Wigand, T. Xu, 2007: Tropical Pacific—mid-latitude teleconnections in medieval times. *Climate Dynamics*, **83**, 241-285.

Gent, P. R., and M. A. Cane, 1989: A reduced gravity, primitive equation model of the upper equatorial ocean. J. Compute. Phys. 81, 444-480.

Gent, P. R., 1991: The heat budget of the TOGA-COARE domain in an ocean model. J Geophys. Res., 96, 3323-3330.

Gent, P.R., F.O. Bryan, G. Danabasoglu, S.C. Doney, W.R. Holland, W. G. Large, and J.C. McWillaims, 1998: The NCAR Climate System Model Global Ocean Component. J. Climate, 11, 1287-1306.

Gu, D. and G. Philander, 1997: Interdecadal Climate Fluctuations that Depend on

Exchanges Between the Tropics and Extratropics, Science, 275, 805-807.

Guilyardi E., A. Wittenberg, A. Fedorov, M. Collins, C. Wang, A. Capotondi, G.J. van Oldenborgh, T. Stockdale 2009: Understanding El Niño in Ocean-Atmosphere General Circulation Models : progress and challenges. Bull. Amer. Met. Soc., published online, in press

Hoerling, M. P., and A. Kumar, 2003: The perfect ocean for drought. Science, 299, 691-694.

Huang, R. and Y. Wu, 1989: The Influence of ENSO on the Summer Climate Change in China and its mechanism. Adv. Atmos. Sci., 6, 21-32.

Huber, M., and R. Caballero 2003: Eocene El Niño: Evidence for Robust Tropical Dynamics in the "Hothouse". Science, 299, 877-881.

IPCC, 2007: IPCC Fourth Assessment Report (http://www.ipcc.ch/ipccreports/ar4-wg1.htm)

Jin, F.F., 1996: Tropical ocean-atmosphere interaction, the Pacific cold tongue, and the El Nino-Southern Oscillation, Science, 274, 76-78.

Jin, F.-F., 1997a: An equatorial ocean recharge paradigm for ENSO. Part I: Conceptual model. J. Atmos. Sci., 54, 811-829.

Jin, F.-F., 1997b: An equatorial ocean recharge paradigm for ENSO. Part II: A stripped-down coupled model. J. Atmos. Sci., 54, 830-847.

Jin F.F., S-I An, A. Timmermann, and J. Zhao, 2003: Strong El Nino events and nonlinear dynamical heating. Geophys. Res. Lett., 30, 1120, DOI:10.1029.

Jones, P.D. and A. Moberg, 2003: Hemispheric and Large-Scale Surface Air Temperature Variations: An Extensive Revision and an Update to 2001. J. Clim., 16, 206-223.

Lin, J.-L., 2007: The Double-ITCZ problem in IPCC AR4 coupled GCMs: Ocean-Atmosphere Feedback Analysis. *J. Climate*, **20**, 4497—4525.

McPhaden M. J. et al., 1998: The tropical ocean-atmosphere observing system, a decade of progress, J. Geophys. Res. 103, 14169--14240.

Kessler, W. S. 2002: Is ENSO a cycle or a series of events?, *Geophys. Res. Lett.*, *29*(23), 2125, doi:10.1029/2002GL015924.

Kirtman, B.P., and P.S. Schopf, 1998: Decadal Variability in ENSO predictability and Prediction. J. Climate, 11, 2804-2822.

Kleeman, R., and S. B. Power, 1994: Limits to predictability in a coupled ocean–atmosphere model due to atmospheric noise. Tellus, 46A, 529–540..

Knutson, T.R., S. Manabe, and D. Gu, 1997: Simulated ENSO in a global coupled ocean-atmosphere model: Multidecadal amplitude modulation and CO2 sensitivity. J. Climate, 10, 131-161.

Lau, K. M., 1985: Elements of a stochastic dynamical theory of the long term variability of the El Niño/Southern Oscillation. J. Atmos. Sci., 42, 1552–1558.

Liu,Z., J. Kutzbach, L. Wu, 2000: Modeling Climate Shift of El Nino Variability in the Holocene. Geophys. Res. Lett. 27, 2265-3368.

Mann, M.E., Z. Zhang, S. Rutherford, R.S. Bradley, M.K. Hughes, D. Schindell, C. Ammann, G. Faluvegi, and F. Ni, 2009: Global Signatures of the "Little Ice Age" and "Medieval Climate Anomaly" and Plausible Dynamical Origins. *Science*, in press.

McPhaden, M.J., S.E. Zebiak, M.H. Glantz, 2006: ENSO as an integrating concept in earth science. Science, 314, 1740-1745.

McCreary, J.P., and P. Lu, 1994: On the interaction between the subtropical and the equatorial oceans: The Subtropical Cell. *J. Phys.Oceanogr.*, **24**, 466-497.

Meehl, G.A., C. COVEY, B. Mcavaney, M. Latif, and R. J. Stouffer, 2005: Overview of the Coupled Model Intercomparison Project. Bull. Amer. Meteor. Soc., 90, 89-93.

Meehl, G.A., P.R., Brantstator, and W.M., Washington, 1993: Tropical Pacific interannual variability and CO2 climate change. J. Climate, 6, 42-63.

Meehl, G.A., P.R. Gent, J. M.Arblaster, B.L. Otto-Bliesner, E.C. Brady, and A. Craig, 2001: Factors that affect the amplitude of El Nino in global coupled climate models. Clim. Dyn., 17, 515-526.

Moy, C. M., G. O. Seltzer, D. T. Rodbell, and D. M. Anderson (2002), Variability of El Niño/Southern Oscillation activity at millennial timescales during the Holocene epoch, Nature, 420, 162–165.

Neale, R. B., J. H. Richter, and M. Jochum, 2008: The impact of convection on ENSO: From a delayed oscillator to a series of events. *J. Climate,* **21,** 5904-5924.

Neelin, J.D., D.S. Battisti, A. C. Hirst, F. F. Jin, Y. Wakata, T. Yamagata, and S. Zebiak, 1998: ENSO Theory. J. Geo. Res., 103, 14261-14290.

Neelin, J.D., and F.F. Jin, 1993: Modes of interannual tropical ocean-atmosphere interaction--a unified view, II: Analytical results in the weak coupling limit. J. Atmos. Sci., 50, 3054-3522.

Newton, A., R. Thunell, and L. D. Stott, 2006: Climate and hydrographic Pacific warm pool during the last millennium. Geophys. Res. Let., 33, doi: 10.1029/2006GL027234.

O'Brien J. J., T. S. Richards, and A. C. Davis, 1996: The effect of El Niño on U.S. landfalling hurricanes. Bull. Amer. Meteor. Soc., 77, 773–774.

Oppo, D.W., Y. Rosenthal, B.K. Linsley, 2009: 2000-year-long temperature and hydrology reconstructions from the Indo-Pacific Warm Pool, *Nature,* **460**, 1113-1116.

Penland, C., and P. D. Sardeshmukh, 1995: The optimal growth of tropical sea surface temperature anomalies, J. Climate, 8, 1999-2024.

Penland, C.; Flügel, M.; P. Chang, 2000: Identification of Dynamical Regimes in an Intermediate Coupled Ocean-Atmosphere Model. J. of Climate, 13, pp.2105-2115.

Penland, C., D.-Z. Sun, and A. Captondi, 2009: An introduction to El Nino and La Nina. This volume.

Pedlosky, J., 1987: An inertial theory of the equatorial undercurrent. *J.Phys. Oceanogr.*,

17, 1978- 1985.

Rasmusson, E., and T. Carpenter, 1982: Variations in tropical sea surface temperature and surface wind fields associated with the Southern Oscillation/El Niño. Mon. Wea. Rev., 110, 354–384.

Ramanatahn V. and W. Collins, 1991: Thermodynamical Regulation of ocean warming by cirrus clouds deduced from observations of the 1987 El Nino. Nature, 351, 27-32.

Rayner, N.A., E.B. Horton, D.E. Parker, C.K. Folland, and R.B. Hackett, 1996: "Version 2.2 of the Global sea-ice and Sea Surface Temperature data set, 1903-1994", September 1996, Climate Research, Technical Note 74 (CRTN74), Hadley Centre for Climate Prediction and Research, Meteorological Office, London Road, Bracknell, Berkshire RG12 2SY.

Rein, B., A. Lückge, and F. Sirocko , 2004: A major Holocene ENSO anomaly during the Medieval period, *Geophys. Res. Lett.,* **31**, L17211, doi:10.1029/2004GL020161.

Rein, B. 2005: El Niño variability off Peru during the last 20,000 years, Paleoceanogr, 20, PA4003, doi:10.1029/2004PA001099.

Rodbell, D. T., G. O., Seltzer, D. M. Anderson, M. B. Abbott, D. B. Enfield, J. H. Newman, 1998: An 15,000-year record of El Niño driven alluviation in southwestern

Ecuador. Science, 283, 516-520.

Ropelewski, C.F., and M.S., Halpert, 1996: Quantifying the Southern Oscillation Precipitation relationships, J.Climate, 9, 1043-1059.

Sachs, J.P., Sachse, D., Smittenberg, R.H., Zhang, Z., Battisti, D.S., Golubic, S., (2009) "Southward movement of the Pacific intertropical convergence zone AD 1400-1850." Nature Geoscience, 2(7): 519-525.

Sandweiss, D.H., J.B., Richardson III, E.J., Reitz, H.B., Rollins, K.A. Maasch, 1996: Determining the early history of El Niño: Response. Science, 273, 1531-1533.

Schneider, N., A. J. Miller, M. A. Alexander, and C. Deser, 1999: Subduction of decadal North Pacific temperature anomalies: Observations and dynamics. Journal of Physical Oceanography, 29, 1056–1070.

Smith, R.S., D.M. Legler, M.J., Rmiigio, J. J., O'Brien, 1999: Comparison of U.S. Temperature and Precipitation anomalies to historical warm phases. J. Climate, 12, 3507-3515.

Suarez, M.J., and Schopf, P., 1988: A delayed action oscillator for ENSO. J. Atmos. Sci, 45, 3283-3287.

Sun, D.Z. 1997: El Niño: A coupled response to radiative heating? Geophys. Res. Lett., 24, 2031-2034.

Sun, D.Z.,2000: Global climate change and ENSO: a theoretical framework. El Niño:

Historical and Paleoclimatic Aspects of the Southern Oscillation, Multiscale variability and Global and Regional Impacts. Cambridge: Cambridge University Press, edited by Diaz H. F. and V. Markgraf, 443-463

Sun, D.Z., 2003: A possible effect of an increase in the warm-pool SST on the magnitude of El Nino warming. J. Climate, 16, 185-205.

Sun, D-Z., 2004: The control of meridional differential surface heating over the level of ENSO activity: a heat-pump hypothesis. Accepted for publication in Ocean-Atmosphere Interaction and Climate Variability, AGU monograph, Edited by C. Wang, S.-P. Xie, and J. Carton.

Sun, D.-Z., 2007: The Role of ENSO in Regulating its Background State. In "Nonlinear Dynamics in Geosciences", pages 537-555, Springer New York, 604 pages, Edited by J. Elsner and A. Tsonis.

Sun, D.-Z., J. Fasullo, T. Zhang, and A. Roubicek, 2003: On the radiative and dynamical feedbacks over the equatorial Pacific cold-tongue. J. Clim., 16, 2425—2432.

Sun, D.-Z., and Z. Liu, 1996: Dynamic ocean-atmosphere coupling: a thermostat for the tropics. Science, 272, 1148-1150.

Sun, D.-Z., T. Zhang, and S.-I. Shin, 2004: The effect of subtropical cooling on the amplitude of ENSO: a numerical study. J. Climate, 17, 3786-3798

Sun. D.Z., and K. E. Trenberth, 1998: Coordinated heat removal from the tropical Pacific

region during the 1986-87 El Niño, Geophys. Res. Lett., 25, 2659-2662.

Sun, D.-Z., T. Zhang, C. Covey,S. Klein, W.D. Collins, J.J. Hack, J.T. Kiehl, G.A. Meehl, I.M. Held, and M. Suarez, 2006 : Radiative and Dynamical Feedbacks Over the Equatorial Cold-tongue: Results from Nine Atmospheric GCMs. J. Climate , 19 , 4059-4074.

Tett, S., 1995: Simulation of El Nino-Southern Oscillation-like variability in a global AOGCM and its response to CO2 increase. J. Climate, 8, 1473-1502.

Timmermann, A., and F.-F. Jin, 2002: A Nonlinear Mechanism for Decadal El Nino Amplitude Changes. Geophys. Res. Lett., 29, Doi: 10.1029/2001GL013369.

Timmermann, A., J. Oberhuber, A. Bacher, M. Esch, M. Latif, and E. Roeckner, 1999: Increased El Niño frequency in a climate model forced by future greenhouse warming. Nature, 398, 694-697.

Timmermann, A., F.F. Jin, and M. Collins, 2004: Intensification of the annual cycle in the tropical Pacific due to greenhouse warming. Geophys. Res. Lett. 31,L12208, doi: 10.1029/2004GL019442.

Trenberth K. E., and T.J. Hoar, 1997: El Nino and Climate Change, Geophys. Res. Lett. 24, 3057-3060

Trenberth, K. E., G. W. Branstator, D. Karoly, A. Kumar, N.-C. Lau, and C. Ropelewski, 1998: Progress during TOGA in understanding and modeling global teleconnections

associated with tropical sea surface temperatures. J. Geophy. Res., 103, 14291-14324.

Trouet,V., J. Esper, N.E.Graham, A. Baker, J. D. Scourse, D. C. Frank, 2009: Persistent Positive North Atlantic Oscillation Mode Dominated the Medieval Climate Anomaly. *Science* **324**, 78-80

Tziperman, E., 1997: Mechanisms of Seasonal-ENSO interaction, J. Atmos. Sci., 54, 61--71

Tudhope, A. W., C. P. Chilcott, M. T. McCulloch, E. R. Cook, J. Chappell, R. M. Ellam, D. W. Lea, J. M. Lough, and G. B. Shimmield, 2001: Variability in the El Niño-Southern Oscillation Through a Glacial-Interglacial Cycle, Science, 291, 1511-1517.

Vecchi, G.A., A. Clement, and B. Soden (2008): Examining the Tropical Pacific's Response to Global Warming. EOS, Trans. Amer. Geophys. Union, 89(9), 81-83.

Wang, C., and J. Picaut, 2004: Understanding ENSO physics--a review. p21-48. In Earth's Climate: The Ocean-Atmosphere Interaction, AGU Geophysical Monograph, Vol. 147, 414 pages. Edited by C. Wang, S.-P. Xie, and J. Carton.

Wang, B., A. Barcilon, and Z. Fang, 1999: Stochastic Dynamics of El Niño–Southern Oscillation*. J. Atmos. Sci., 56, 5–23..

Wang, B., J. Yang, T. Zhou, and B. Wang, 2008: Interdecadal Changes in the Major

Modes of Asian–Australian Monsoon Variability: Strengthening Relationship with ENSO since the Late 1970s. J. Climate, 21, 1771–1789

Wolter, K., R. M. Dole, and C. A. Smith, 1999: Short-Term Climate Extremes over the Continental United States and ENSO. Part I: Seasonal Temperatures. J. of Climate, 12, 3255-3272.

Wyrtki, K. 1985: Water displacements in the Pacific and the genesis of El Nino cycles. J. Geophys. Res., 90, 7129-7132.

Zebiak, S. E., and M. A. Cane, 1987: A model El Niño Southern Oscillation. Mon. Wea. Rev., 115, 2262-2278.

Zhang,T.,D.-Z. Sun, R. Neal, and P. Rasch, 2008: An Evaluation of ENSO Asymmetry in the Community Climate System Models: A View from the Subsurface. J.Climate, Submitted.

Zhang, Y., J.M.Wallace, and D.S. Battisti, 1997: ENSO-like interdecadal variability. J. Climate, 10, 1004-1020.

Table Legends:

Table 1: Response of Tw, Tc, and Tw-Tc to an enhanced tropical heating with and without ENSO. The definitions of Tw and Tc are the same as in Sun et al. (2004). The three pairs presented here differ in the meridional extent of the regions where an enhanced tropical heating is applied. Anomalous heating is confined to 5^{o}S-5^{o}N for Pair I, 10^{o}S-10^{o}N for Pair II, and 15^{o}S-15^{o}N for Pair III. In all three cases, the increase in the radiative convective equilibrium SST (SSTp) peaks at the equator with a value of 2^{o}C, and then decrease with latitude following a cosine profile to zero at the specified latitudes (i.e., 5^{o}, 10^{o}, and 15^{o} respectively for the three cases). The last 23 years of a 27-year-long run are used in the calculation for the case with ENSO. For the case without ENSO, the last 3 years of data of a 27-year-long run are used in the calculation because there is little interannual variability in this case.

Figure Legends:

Figure 1: (a): Schematic diagram for the coupled model. Solid arrows represent the zonal branch of the equatorial wind-driven circulation constituted by the upwelling in the east Pacific, the westward surface drift, and the equatorial undercurrent. The thermodynamical effect of the atmosphere is to heat the ocean to a zonally uniform SST (Tw) if not opposed by ocean transport (See Eqs. (6) and (7) in Sun 2000). (Tw has been called the radiative convective equilibrium SST and may be regarded as the tropical maxiumum SST or the SST of the warmpool). T_c represents the characteristic temperature of the equatorial undercurrent. T_{sub} is the temperature of the water that actually enter the surface mixed layer in the eastern Pacific. The dashed arrow represents the surface winds. (b) and (c): Oscillations at Tw=29.5^{o}C, a value corresponding to the maximum SST of the observed climate. (b): variations of T_1 and T_2. (c): variations of h_2 (anomaly of the thermocline depth in the eastern Pacific). The dashed line is anomalies of T_2

Figure 2: (a) Equilibrium solutions of the coupled system as a function of Tw. The value for Tc is fixed at 17.3^{o}C. The corresponding differences between Tw and Tc are also

marked in the figure. Dashed lines indicate that the solution exists, but unstable (b) Amplitude of Oscillation as a function of Tw. For more details, see Sun (1997).

Figure 3: A schematic showing the extended conceptual model (a), equilibrium SST of the coupled system as a function of T_3 (b), and amplitude of the oscillation as a function of T_3 (c). Warm pool temperature T_w is fixed at 29.5 ^{o}C. as the value T_3 is varied.

Figure 4: Response of ENSO to an increase in the tropical heating (a) and subtropical/extratropical cooling (b). Shown are time series of Niño3 SST from a control run (solid line) and a perturbed run (dashedline) in which the restoring convective equilibrium temperature (SST_p) is either increased in to a higher value over the tropics (tropical heating case) or reduced to a lower value over the extratropics (extratropical cooling case). See Sun et al. (2004) for more details.

Figure 5: Time-mean equatorial upper ocean temperature response to an enhanced tropical heating for the case without ENSO (a) and the case with ENSO (b). Shown are the results from experiments of Pair II listed in Table 1. Data used for the

calculations here are the same as used for obtaining changes in Tw and Tc in Table 1. The thin dashed contours indicate the mean isentropes of the control run.

Figure 6: Differences in the equatorial upper ocean temperature between the perturbed run and the control run during the La Niña phase (a) and during the El Niño phase (b). The results are from pair II (see legends of Table 1). The 6 cycles of the last 23-years of a 27-year-long run are used in this calculation.

Figure 7: Time-mean equatorial upper ocean temperature response to an enhanced extratropical cooling for the case without ENSO (a) and the case with ENSO (b). Anomalous extratropical cooling—a reduction in SSTp—starts at 10^{o} S(N) for this case and increases monotonically with latitude to a fixed value 1^{o}C at 30^{o}S(N). The last 3 years of data of a 27-yr-long run are used in the calculation for the case without ENSO. For the case with ENSO, the last 23 years of a 40-year long run are used. Not like the almost instantaneous response of ENSO to an increase in the tropical heating, there is a delay for the onset of the regime with stronger ENSO in response to an increase in extratropical cooling. Consequently there is a need for a longer run to obtain a time series of Niño3 SST that is representative of the regime.

Figure 8: Response of the upper ocean temperature to extratropical cooling with and without ENSO. Shown are the zonal mean values.

Figure 9: Differences in the equatorial upper ocean temperature between the perturbed run and the control run during the La Niña phase (a) and during the El Niño phase (b) for the enhanced extratropical cooling experiment. Data used are the same as for the case with ENSO in Fig. 7.

Figure 10: Equatorial upper ocean temperature from a run with constant wind (a) and a run with interannually varying wind (b). The time-mean wind stresses are the same as both runs (the 1950-1999 mean wind stress from NCEP). So are the thermal boundary conditions: both runs are restored to the same radiative convective equilibrium SST.

Figure 11: (a) difference in the equatorial upper ocean temperature between the run with constant wind and the run with fluctuating wind. (b) same as (a) except the fluctuation part of the wind is amplified by 50%.

Figure 12: Nino3 SST (anomalies) (in color). The black solidline is the variance of Nino3 SST anomalies obtained by sliding a moving window of a width of 16 years.

Figure 13. The upper panel shows the time series of subsurface temperature in the equatorial eastern (red) and western Pacific (black). The bottom panel is the difference between the two.

Figure 14: The time series of tropical maximum SST that corresponds to the Nino3 SST time series shown in Fig. 12 (upper panel). The SST trends over the last three decades (1976-2006) (lower panel).

Figure 15: Time series of Tc, defined here as the average equatorial subsurface temperature in the region (100m-225m, 160E-220E, 5S-5N) (upper panel). The trend in the equatorial upper ocean temperature over the last 30 years (lower panel).

Figure 16: The evolution of Tw-Tc over the last 50 years. Note the elevated state in the last 30 years.

Figure 17. (Top) SST records in the western equatorial Pacific (red line) and in the eastern equatorial Pacific (blue and green). (Bottom) Alkenone-based SST records for the California margin (black), the Peru margin (blue), and the West African margin (green). (From Fedorov et al. (2006)).

Figure 18. Downcore lithic concentrations at site 106 KL (MCA - Medieval climate anomaly) (From Rein et al. 2004).

Figure 19. a, The MBH Northern Hemisphere temperature reconstruction (green) plotted with the Northern Hemisphere instrumental temperature record (red). The green horizontal line denotes the mean of the MBH record for the period ad 1886–1975. b. The monthly resolved Palmyra coral ^{18}O records (thin black line), shown with a 10-yr running average (thick yellow line). The black horizontal line represents the average of the Palmyra modern coral ^{18}O for the period ad 1886–1975. c, Reconstruction of solar irradiance anomalies based on historical sunspot records (anomalies calculated with respect to the ad 1886–1975 mean) (purple) plotted with ^{10}Be anomalies (a proxy for solar activity) (blue), plotted as a 3-point running mean and scaled to the solar irradiance anomalies. d, Radiative forcing associated with volcanic eruptions

recorded in ice cores (black). The approximate timing and duration of the 'Little Ice Age' (LIA), the 'Medieval Warm Period' (MWP), and solar activity minima—the Maunder minimum (MM), the Spörer minimum (SP), and the Wolfe minimum (WM)—are marked by horizontal bars (From Cobb et al. 2004).

Figure 20: (a) Standard variations and skewness of Nino3 SST for observations and various versions of NCAR models (b) Stand variations and skewness of subsurface temperature in the eastern Pacific for observations and various versions of NCAR models. Note that although measured by the standard variation, ENSO is as strong or even stronger than the observations, ENSO is weaker in all models than in the observations measured by the skewness.

Figure 21: Scatter diagrams showing the relationship between SST and the cloud albedo (a), and the relationship between SST and precipitation. Data are interannual anomalies averaged over the equatorial Pacific (150E-250E, 5S-5N). The color dots are for the various models, and the black dotes are for the real world (see Sun et al. 2009 for more details).

Figure 22: From top to bottom: (1) response in the mean SST to a 1 K increase in the restoring SST, (2) response in the mean to a 1 K decrease in the restoring SST, (3) time series of Nino3 SST from a control run, (4) time series of Nino3 SST when the restoring SST is increased by 2 K, (5) time series of Nino3 SST when the restoring SST is lowed by 1 K. (From Clement et al. 1996)

perturbation type	experiment type	change of Tw (°c)	change of Tc (°c)	change of Tw-Tc (°c)
Pair I (5°S-5°N)	No ENSO	1.03	0.0050	1.02
	With ENSO	0.81	0.76	0.053
Pair II (10°S-10°N)	No ENSO	1.38	0.036	1.34
	With ENSO	0.97	0.83	0.14
Pair III (15°S-15°N)	No ENSO	0.95	0.24	0.71
	With ENSO	0.55	0.63	-0.085

Table 1: Time-mean response of warmppool SST (Tw), temperature of the equatorial undercurrent (Tc), and their difference (Tw-Tc) to an enhanced tropical heating with and without ENSO. The value of Tw and Tc are calculated the same way as in Sun et al. (2004). The three pairs presented here differ in the meridional extent of the regions where an enhanced tropical heating is applied. Anomalous heating is confined to 5°S-5°N for Pair I, 10°S-10°N for Pair II, and 15°S-15°N for Pair III. In all three cases, the increase in the radiative convective equilibrium SST (SSTp) peaks at the equator with a value of 2°C, and then decrease with latitude following a cosine profile to zero at the specified latitudes (i.e., 5°, 10°, and 15° respectively for the three cases). The last 23 years of a 27-year-long run are used in the calculation for the case with ENSO. For the case without ENSO, the last 3 years of data of a 27-year-long run are used in the calculation because there is little interannual variability in this case.

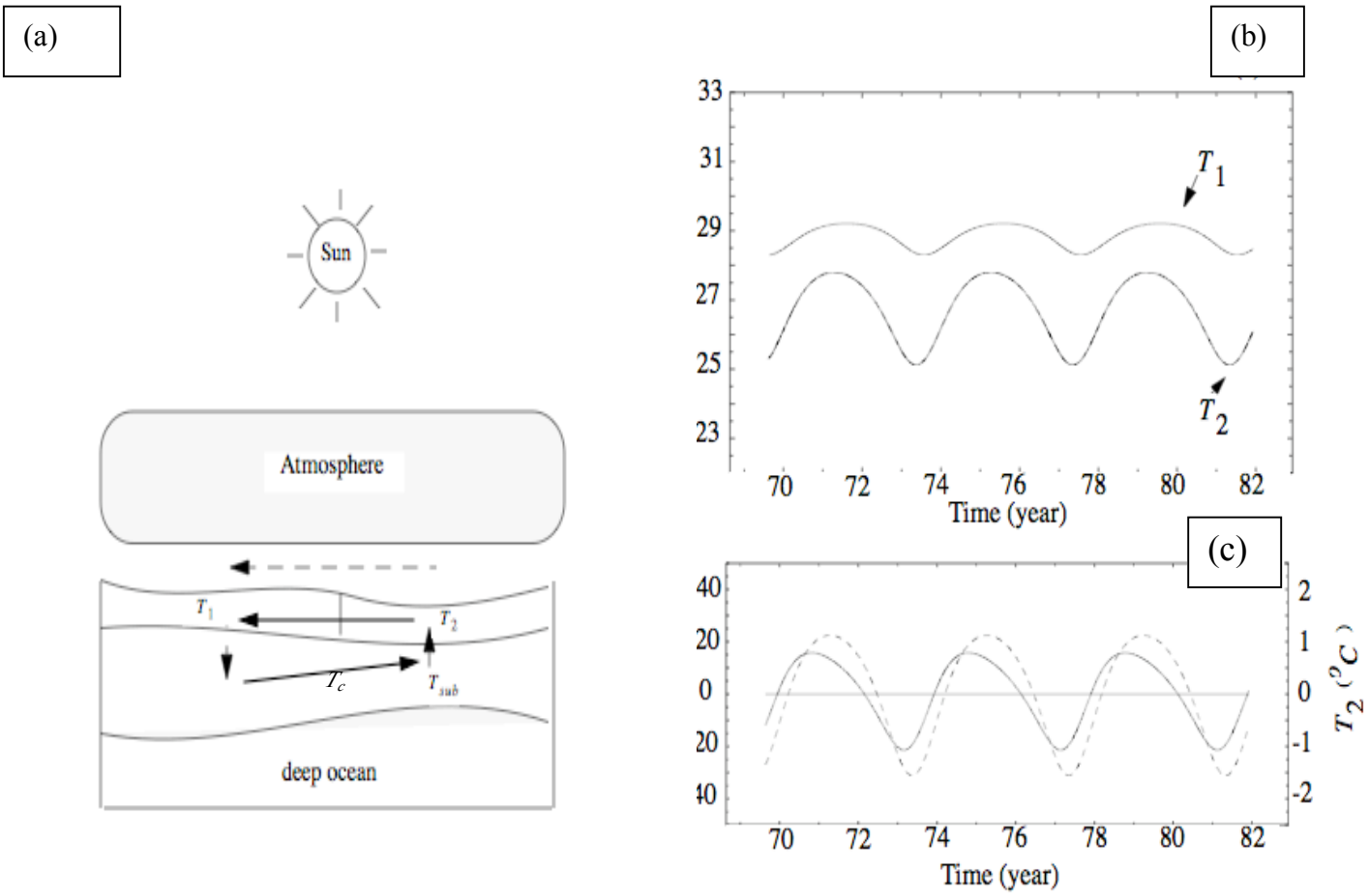

Figure 1: (a): Schematic diagram for the coupled model. Solid arrows represent the zonal branch of the equatorial wind-driven circulation constituted by the upwelling in the east Pacific, the westward surface drift, and the equatorial undercurrent. The thermodynamical effect of the atmosphere is to heat the ocean to a zonally uniform SST (Tw) if not opposed by ocean transport (See Eqs. (6) and (7) in Sun 2000). (Tw has been called the radiative convective equilibrium SST and may be regarded as the tropical maxiumum SST or the SST of the warmpool). T_c represents the characteristic temperature of the equatorial undercurrent. T_{sub} is the temperature of the water that actually enter the surface mixed layer in the eastern Pacific. The dashed arrow represents the surface winds. (b) and (c): Oscillations at Tw=29.5°C, a value corresponding to the maximum SST of the observed climate. (b): variations of T_1 and T_2. (c): variations of h_2 (anomaly of the thermocline depth in the eastern Pacific). The dashed line is anomalies of T_2

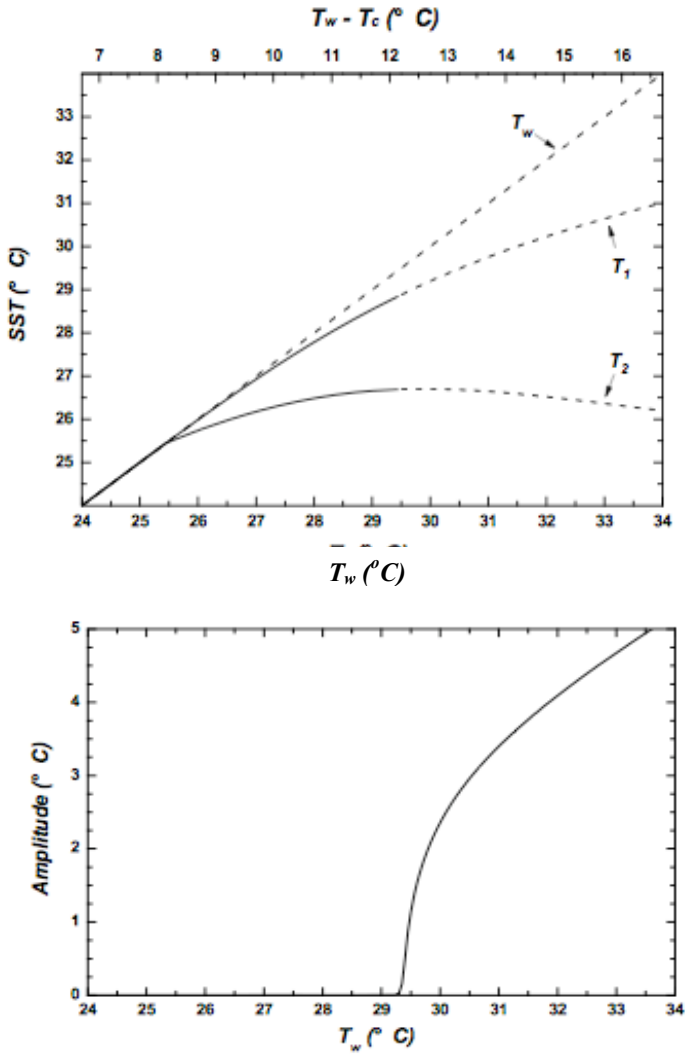

(a)

(b)

Figure 2: (a) Equilibrium solutions of the coupled system as a function of Tw. The value for Tc is fixed at 17.3°C. The corresponding differences between Tw and Tc are also marked in the figure. Dashed lines indicate that the solution exists, but unstable (b) Amplitude of Oscillation as a function of Tw. For more details, see Sun (1997).

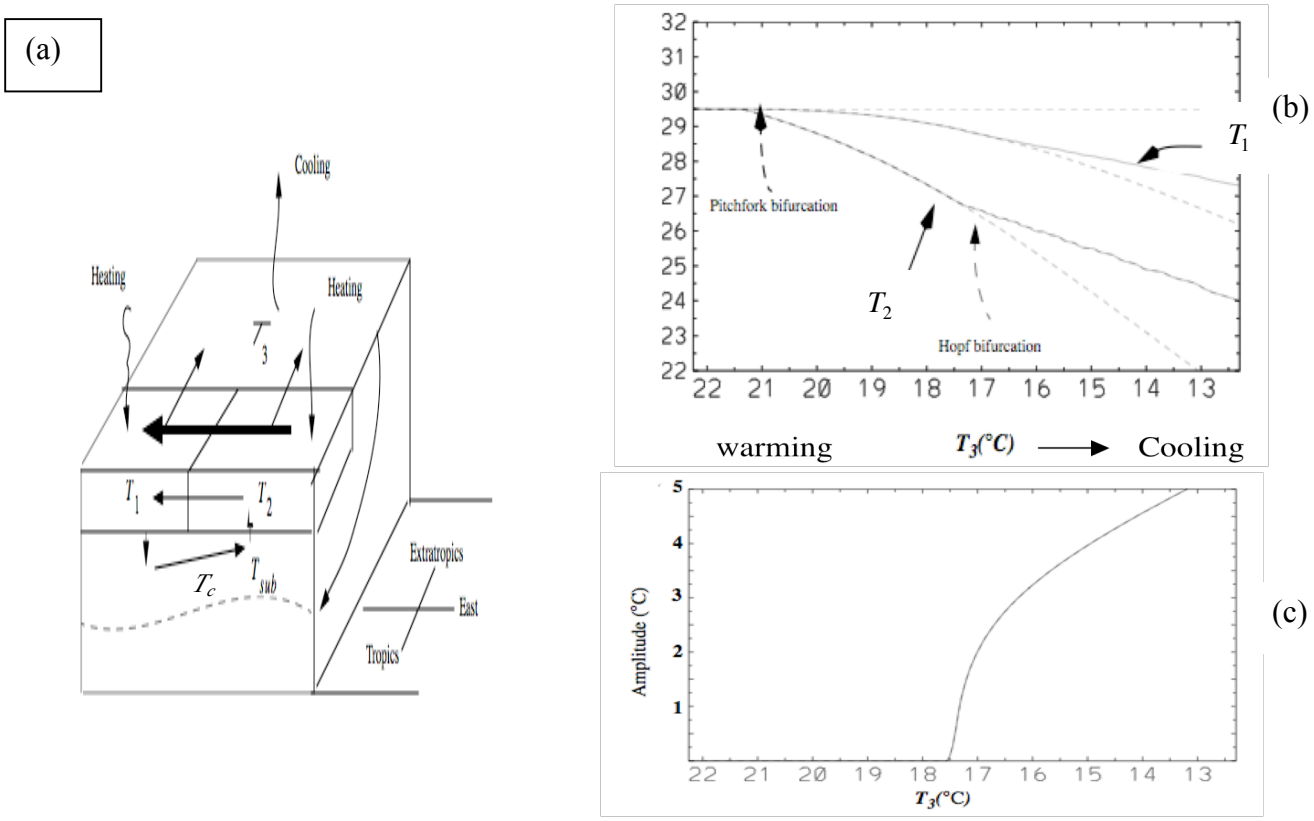

Figure 3: (a) A schematic showing the extended conceptual model. Through subduction process, the temperature of the equatorial undercurrent is directly linked to the extratropical SST (T_3). The equations governing the equatorial SST and the depth of the equatorial thermocline are the same as those for the model shown in Fig. 1a. Equilibrium SST of the coupled system as a function of T_3 (b); Amplitude of the oscillation as a function of T_3 (c). Warm pool temperature T_w is fixed at 29.5 ^{o}C as the value of T_3 is varied.

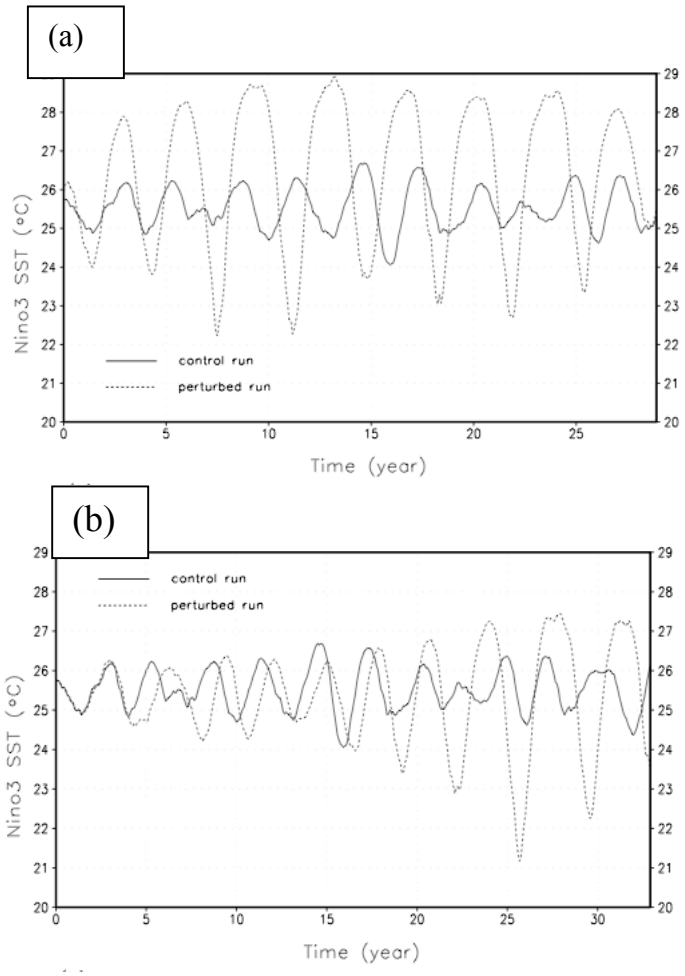

Figure 4: Response of ENSO to an increase in the tropical heating (a) and extratropical cooling (b). Shown are time series of Niño3 SST from a control run (solid line) and a perturbed run (dashedline) in which the restoring convective equilibrium temperature (SST_p) is either increased in to a higher value over the tropics (tropical heating case) or reduced to a lower value over the extraropics (extratropical cooling case). See Sun et al. (2004) for more details.

(a) (b)

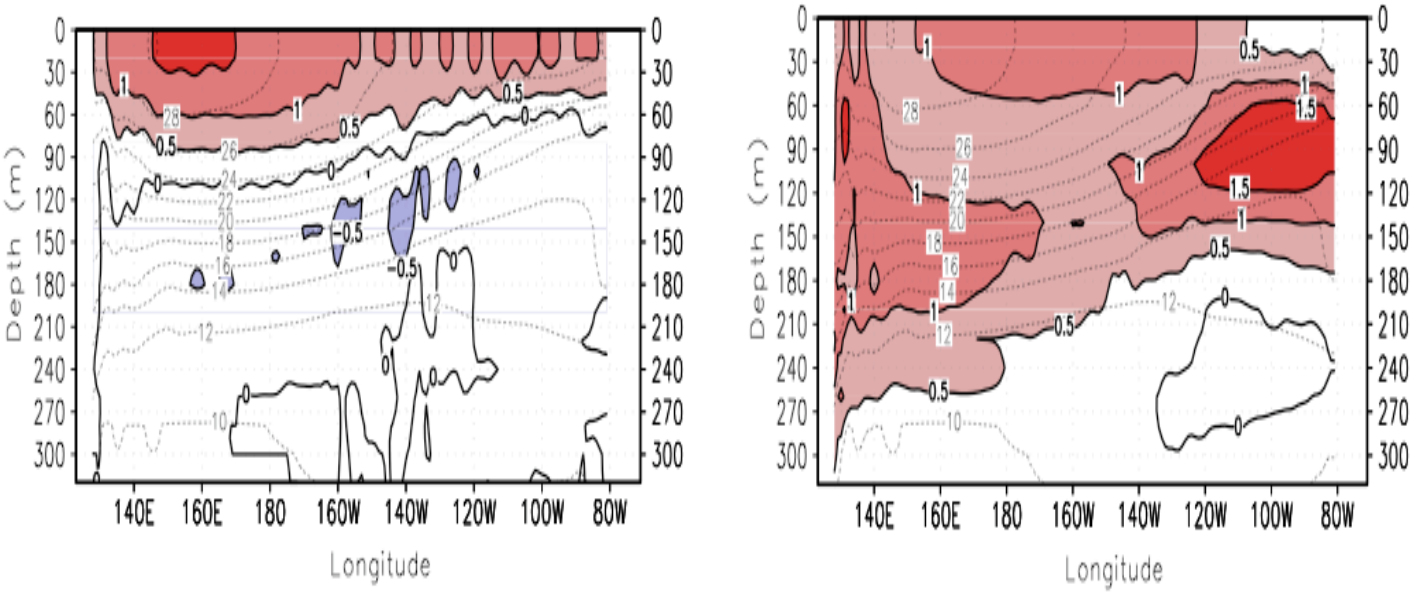

Figure 5: Time-mean equatorial upper ocean temperature response to an enhanced tropical heating for the case without ENSO (a) and the case with ENSO (b). Shown are the results from experiments of Pair II listed in Table 1. Data used for the calculations here are the same as used for obtaining changes in Tw and Tc in Table 1. The thin dashed contours indicate the mean isentropes of the control run.

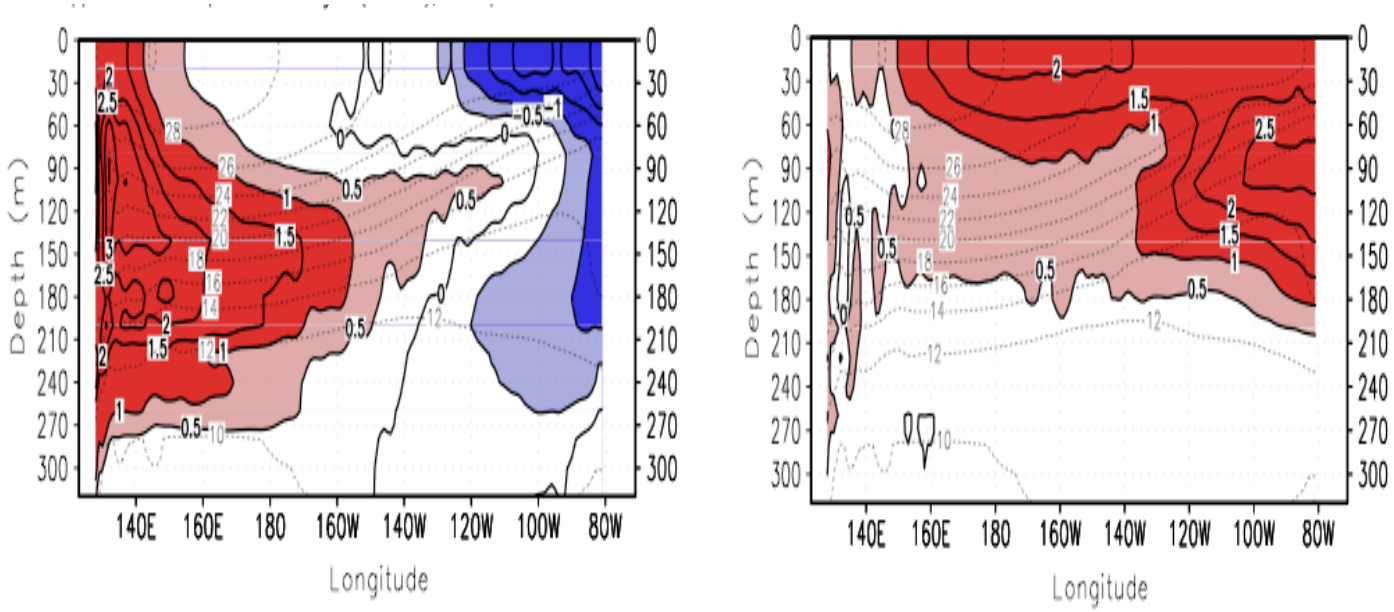

Figure 6: Differences in the equatorial upper ocean temperature between the perturbed run and the control run during the La Niña phase (a) and during the El Niño phase (b). The results are from pair II (see legends of Table 1). The 6 cycles of the last 23-years of a 27-year-long run are used in this calculation

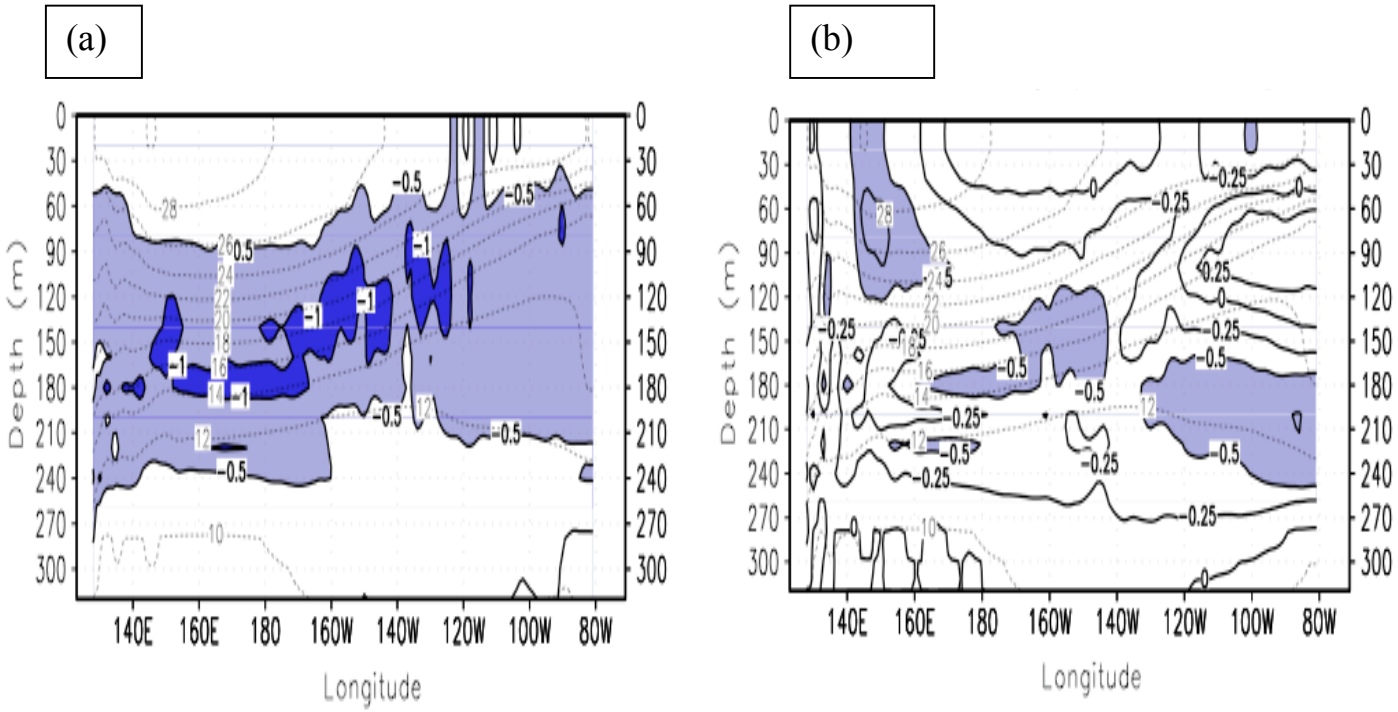

Figure 7: Time-mean equatorial upper ocean temperature response to an enhanced extratropical cooling for the case without ENSO (a) and the case with ENSO (b). Anomalous extratropical cooling—a reduction in SSTp—starts at 10^{o} S(N) for this case and increases monotonically with latitude to a fixed value 1^{o}C at 30^{o}S(N). The last 3 years of data of a 27-yr-long run are used in the calculation for the case without ENSO. For the case with ENSO, the last 23 years of a 40-year long run are used. Not like the almost instantaneous response of ENSO to an increase in the tropical heating, there is a delay for the onset of the regime with stronger ENSO in response to an increase in extratropical cooling. Consequently there is a need for a longer run to obtain a time series of Niño3 SST that is representative of the regime.

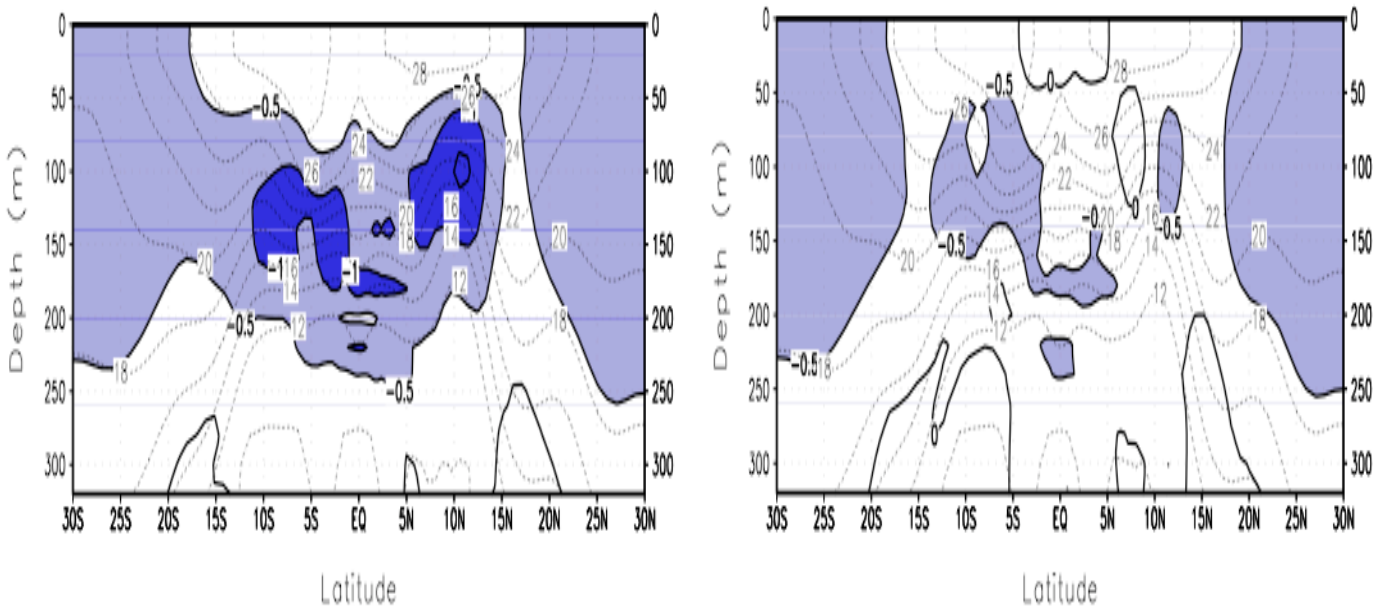

Figure 8: Response of the upper ocean temperature to extratropical cooling with and without ENSO. Shown are the zonal mean values.

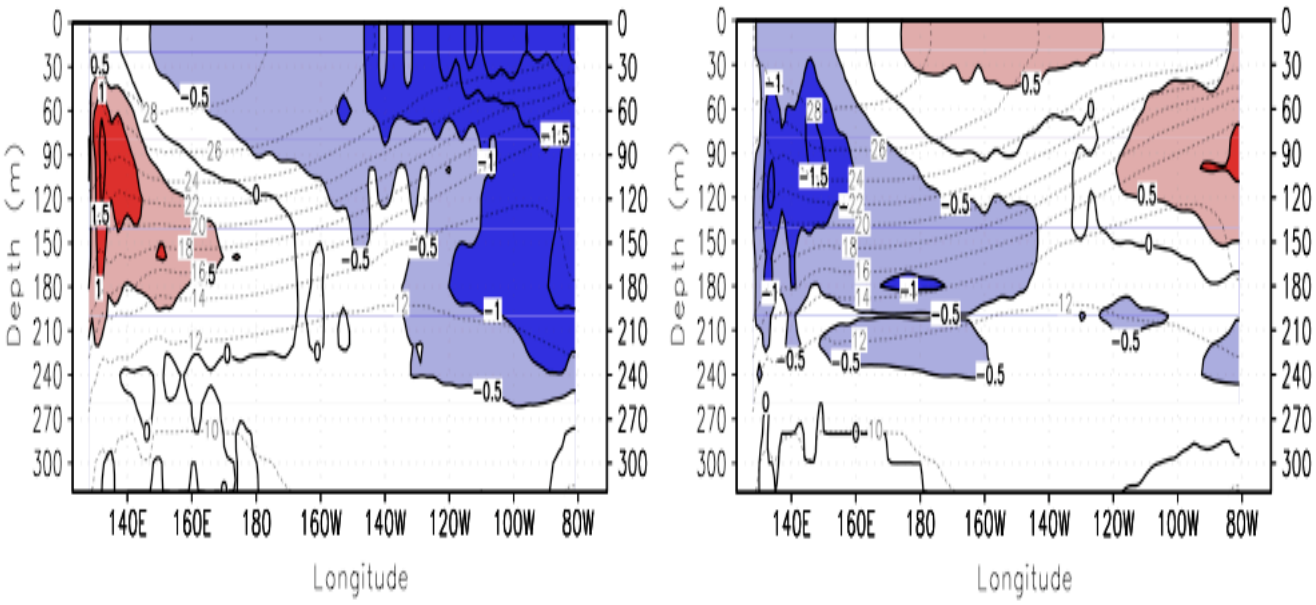

Figure 9: Differences in the equatorial upper ocean temperature between the perturbed run and the control run during the La Niña phase (a) and during the El Niño phase (b) for the enhanced extratropical cooling experiment. Data used are the same as for the case with ENSO in Fig. 7.

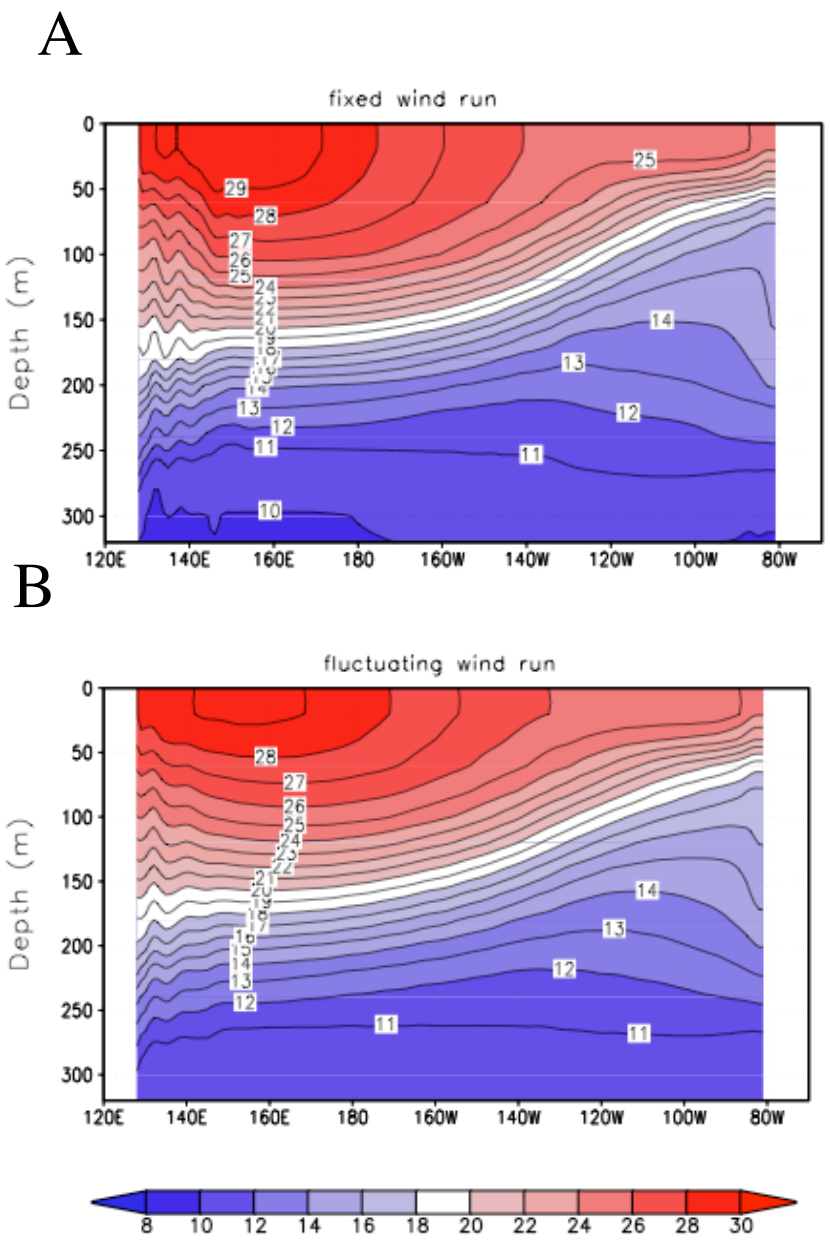

Figure 10: Equatorial upper ocean temperature from a run with constant wind (a) and a run with interannually varying wind (b). The time-mean wind stresses are the same as both runs (the 1950-1999 mean wind stress from NCEP). So are the thermal boundary conditions: both runs are restored to the same radiative convective equilibrium SST.

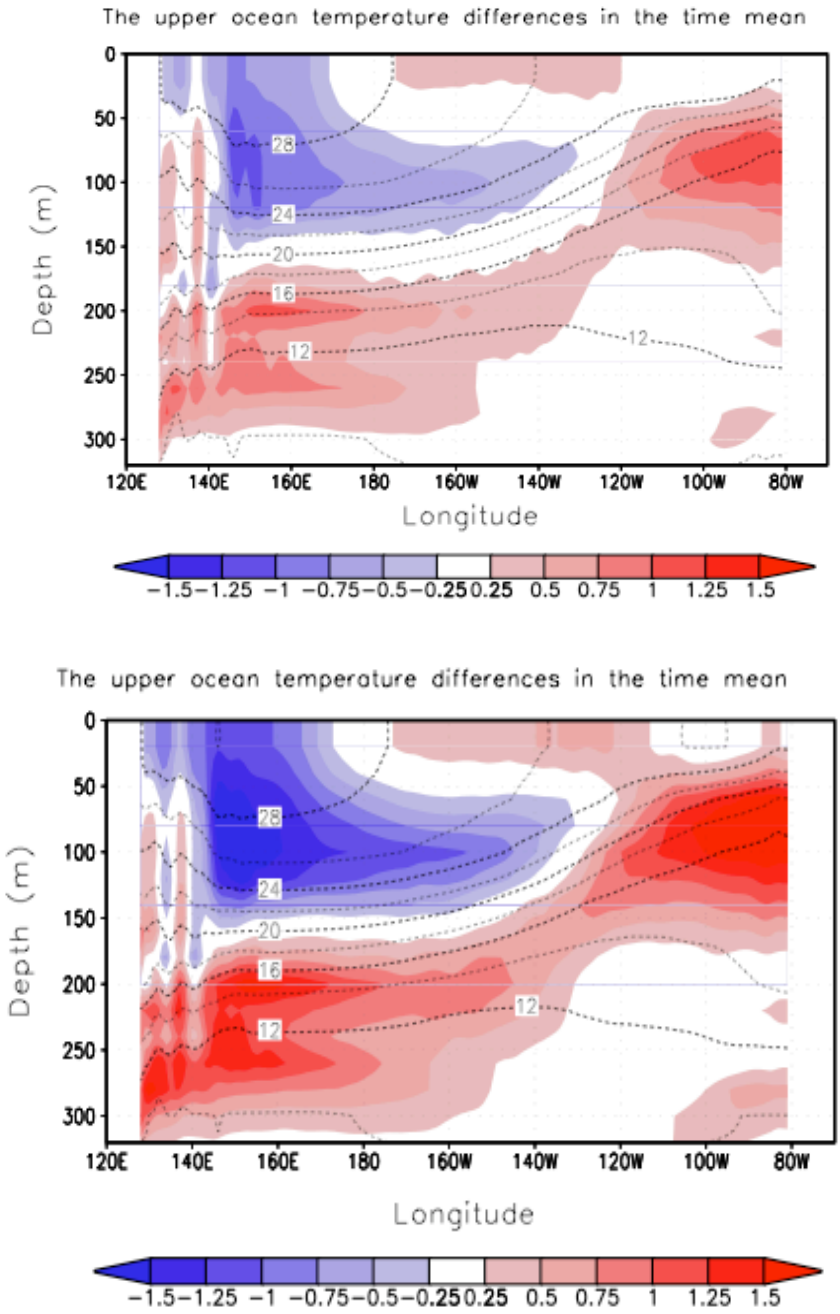

Figure 11: (a) difference in the equatorial upper ocean temperature between the run with constant wind and the run with fluctuating wind. (b) same as (a) except the fluctuation part of the wind is amplified by 50%.

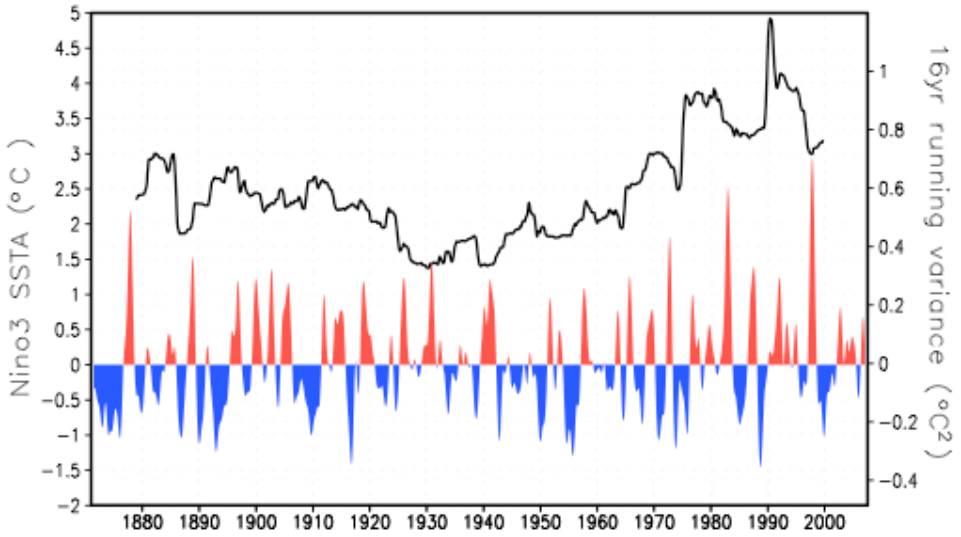

Figure 12: Nino3 SST (anomalies) (in color). The black solidline is the variance of Nino3 SST anomalies obtained by sliding a moving window of a width of 16 years.

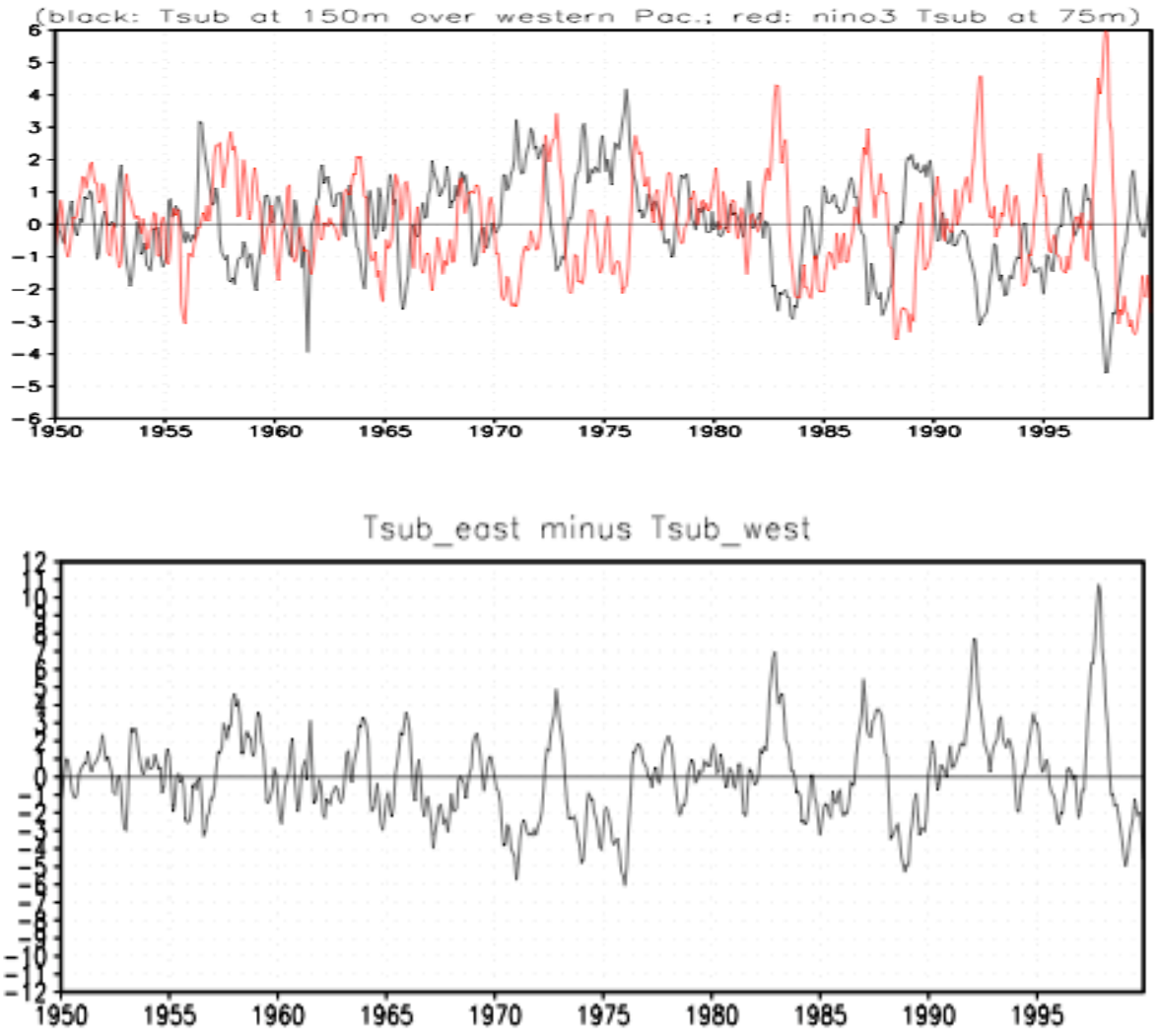

Figure 13. The upper panel shows the time series of subsurface temperature in the equatorial eastern (red) and western Pacific (black). The bottom panel is the difference between the two temperatures.

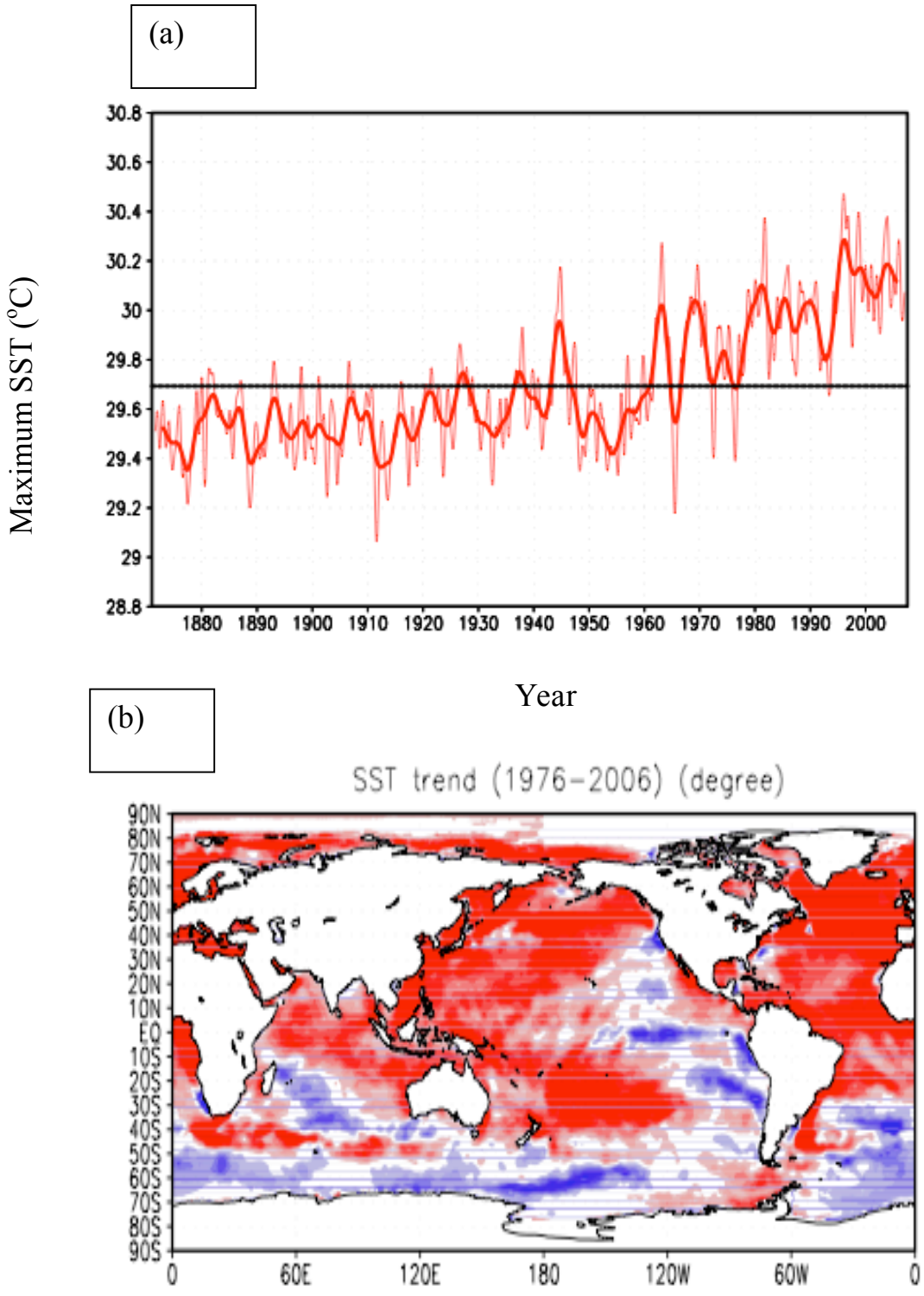

Figure 14: The time series of tropical maximum SST that corresponds to the Nino3 SST time series shown in Fig. 12 (upper panel). The SST trends over the last three decades (1976-2006) (lower panel).

(a)

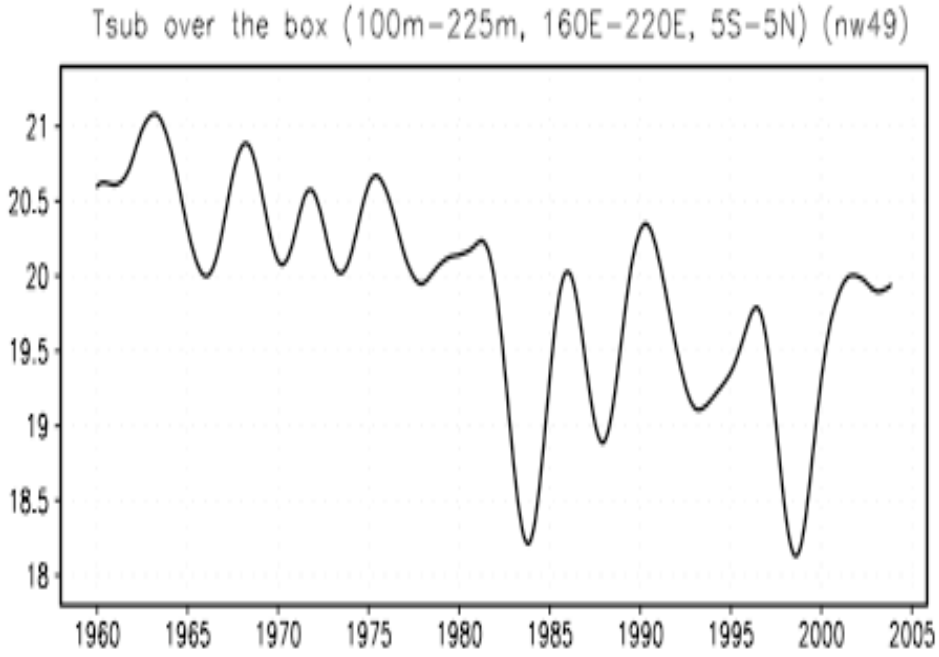

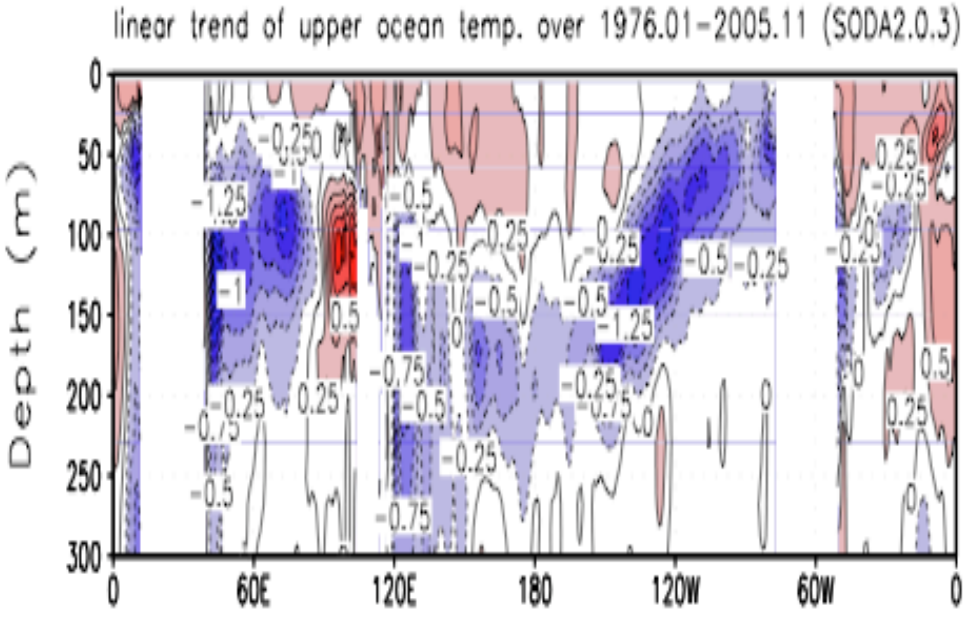

(b)

Figure 15: Time series of Tc, defined here as the average equatorial subsurface temperature in the region (100m-225m, 160E-220E, 5S-5N) (upper panel). The trend in the equatorial upper ocean temperature over the last 30 years (lower panel).

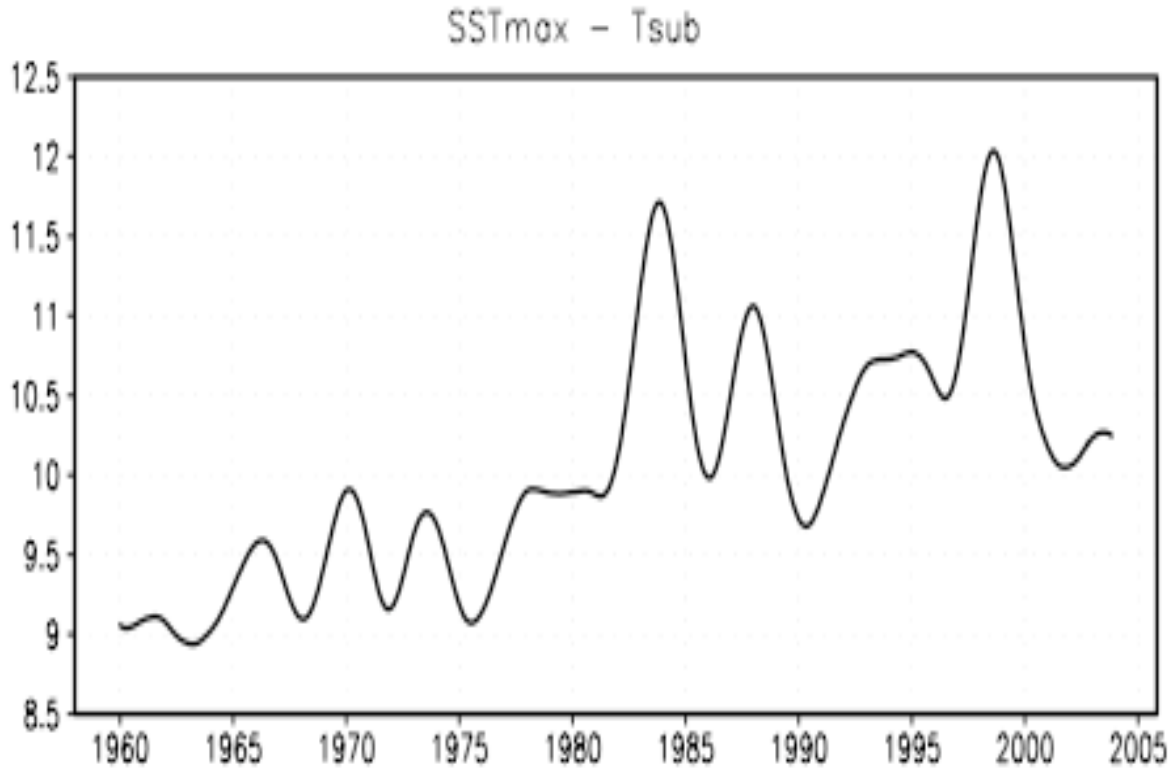

Figure 16: The evolution of Tw-Tc over the last 50 years. Note the elevated state in the last 30 years.

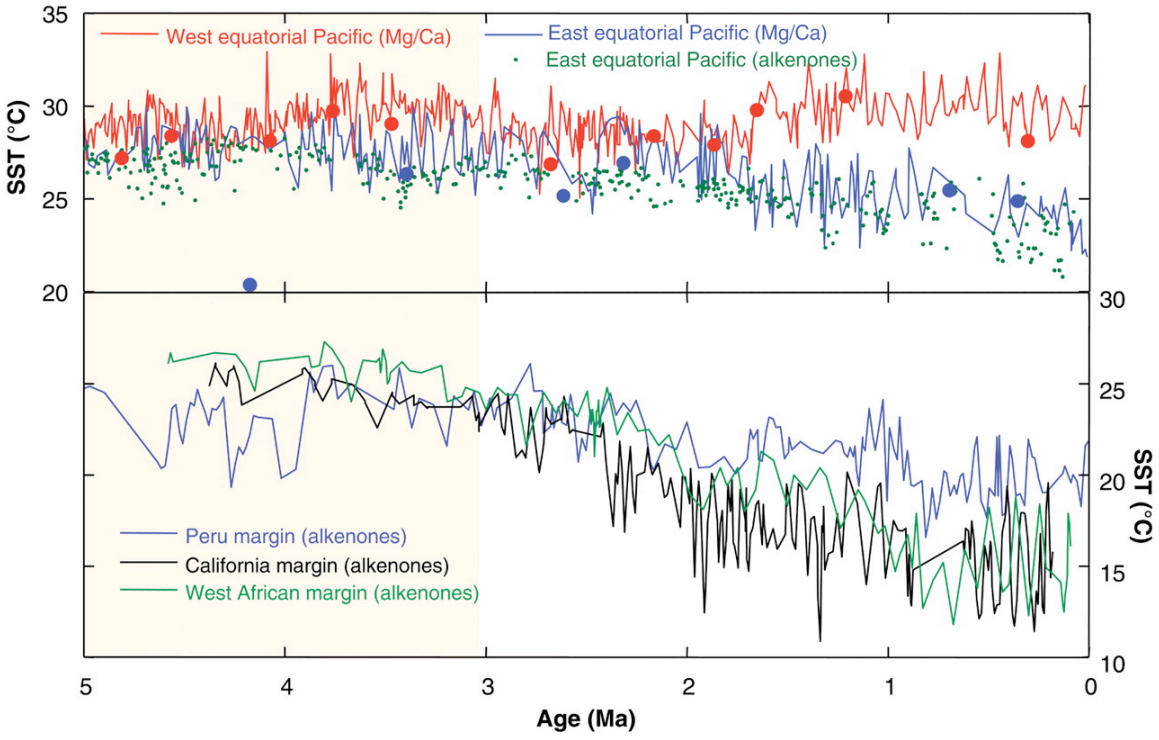

Figure 17. (Top) SST records in the western equatorial Pacific (red line) and in the eastern equatorial Pacific (blue and green). (Bottom) Alkenone-based SST records for the California margin (black), the Peru margin (blue), and the West African margin (green). (From Fedorov et al. (2006)).

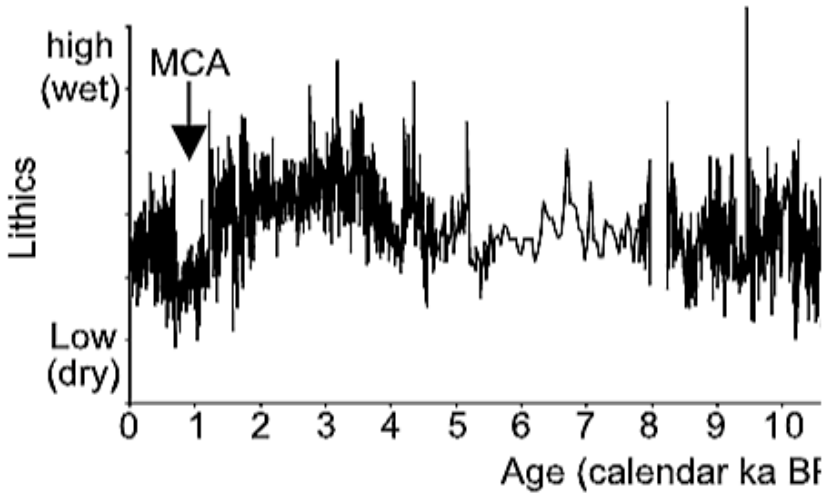

Figure 18. Downcore lithic concentrations at site 106 KL (MCA - Medieval climate anomaly) (From Rein et al. 2004).

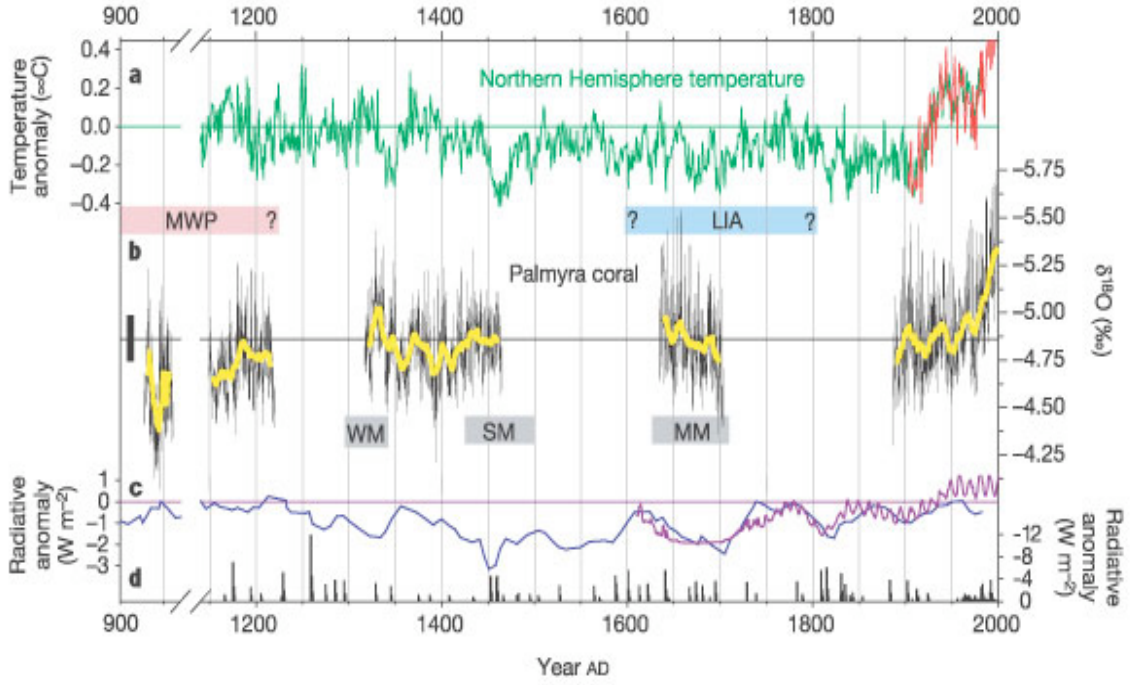

Figure 19. a, The MBH Northern Hemisphere temperature reconstruction (green) plotted with the Northern Hemisphere instrumental temperature record (red). The green horizontal line denotes the mean of the MBH record for the period ad 1886–1975. b. The monthly resolved Palmyra coral ^{18}O records (thin black line), shown with a 10-yr running average (thick yellow line). The black horizontal line represents the average of the Palmyra modern coral ^{18}O for the period ad 1886–1975. c, Reconstruction of solar irradiance anomalies based on historical sunspot records (anomalies calculated with respect to the ad 1886–1975 mean) (purple) plotted with ^{10}Be anomalies (a proxy for solar activity) (blue), plotted as a 3-point running mean and scaled to the solar irradiance anomalies. d, Radiative forcing associated with volcanic eruptions recorded in ice cores (black). The approximate timing and duration of the 'Little Ice Age' (LIA), the 'Medieval Warm Period' (MWP), and solar activity minima—the Maunder minimum (MM), the Spörer minimum (SP), and the Wolfe minimum (WM)—are marked by horizontal bars (From Cobb et al. 2004)

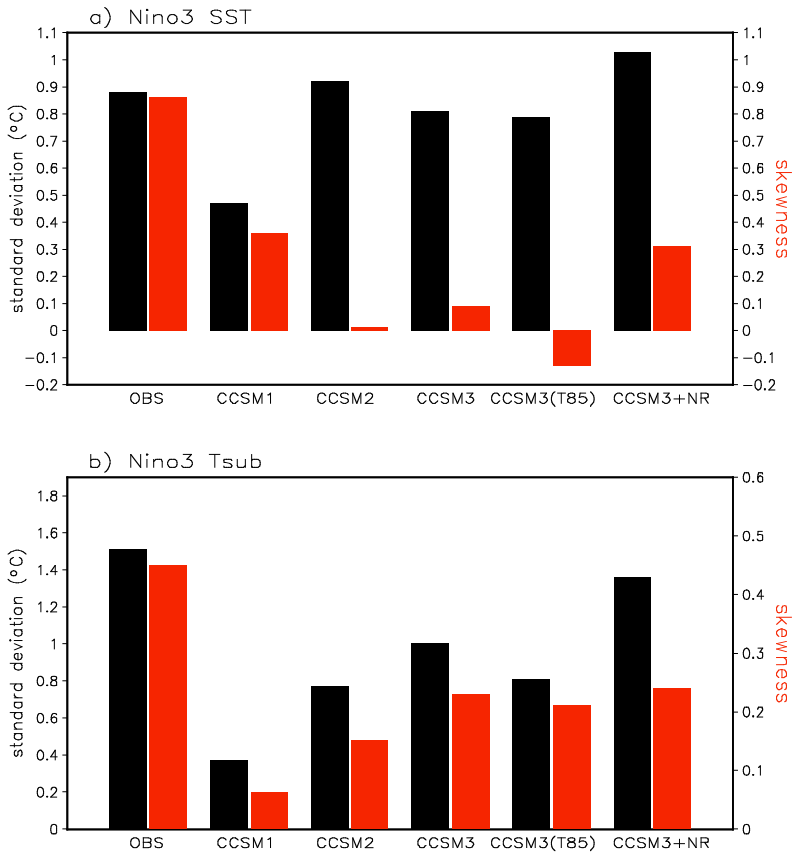

Figure 20: (a) Standard variations and skewness of Nino3 SST for observations and various versions of NCAR models (b) Stand variations and skewness of subsurface temperature in the eastern Pacific for observations and various versions of NCAR models. Note that although measured by the standard variation, ENSO is as strong or even stronger than the observations, ENSO is weaker in all models than in the observations measured by the skewness.

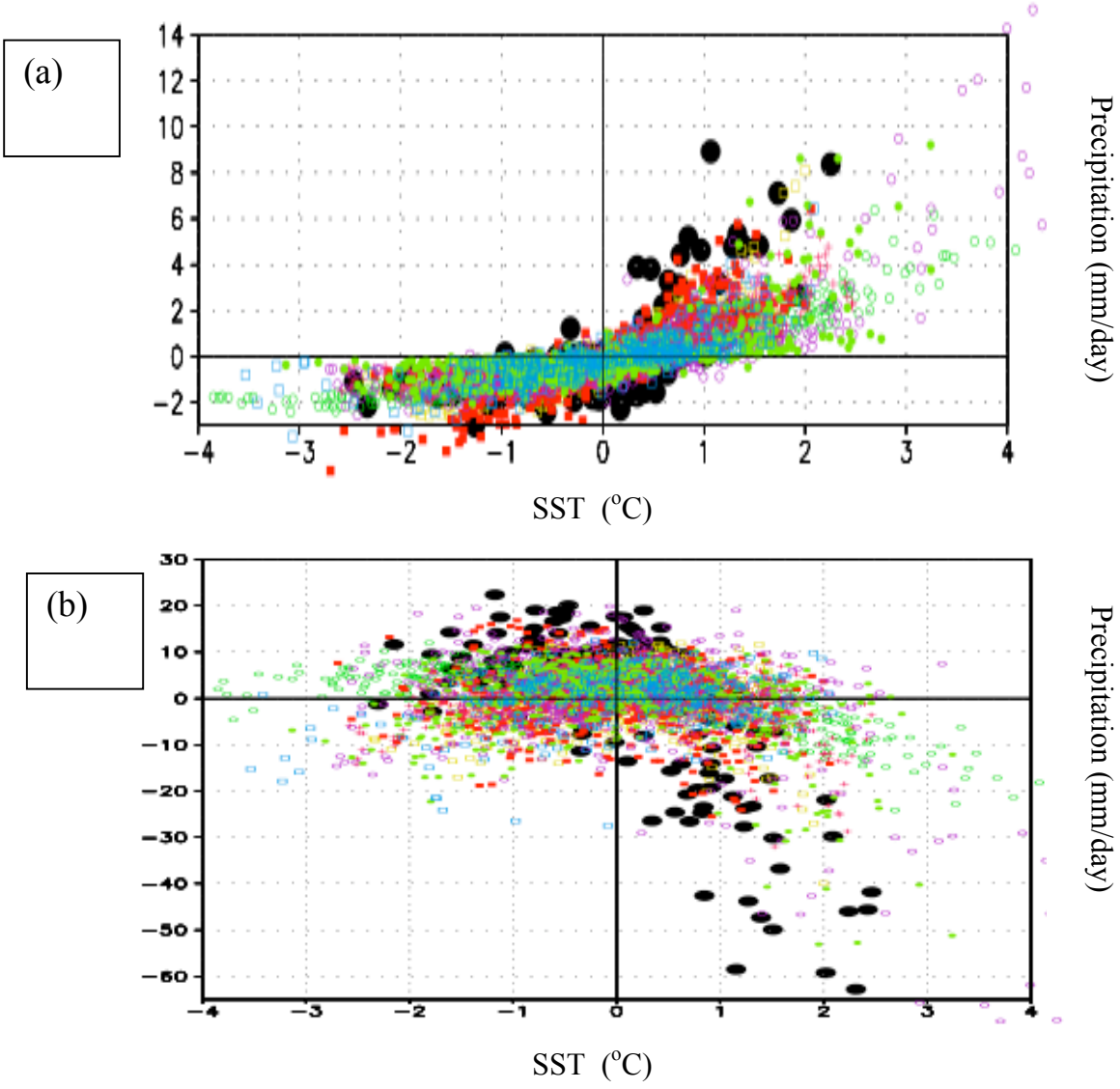

Figure 21: Scatter diagrams showing the relationship between SST and the precipitation (a), and the relationship between SST and cloud albedo (b). Data are interannual anomalies averaged over the equatorial Pacific (150E-250E, 5S-5N). The color dots are for the various models, and the black dotes are for the real world (see Sun et al. 2009 for more details).

(1)

(2)

(3)

(4)

(5)

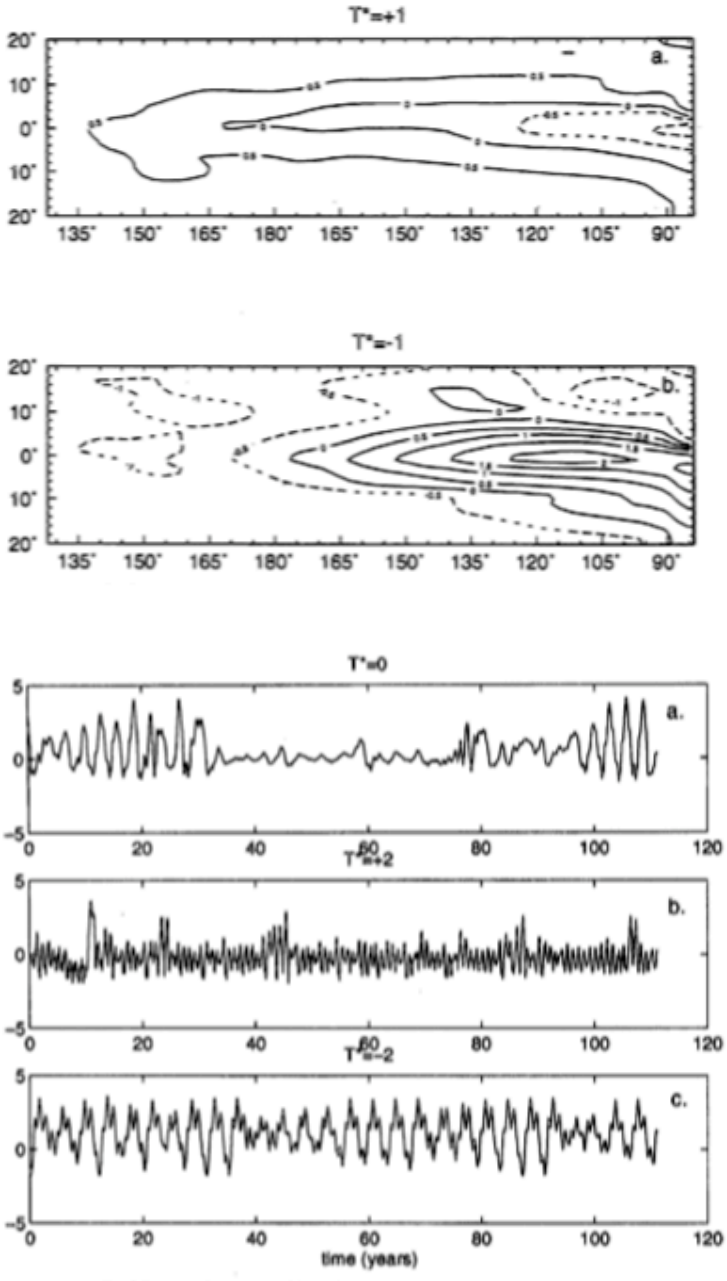

Figure 22: From top to bottom: (1) response in the mean SST to a 1 K increase in the restoring SST, (2) response in the mean to a 1 K decrease in the restoring SST, (3) time series of Nino3 SST from a control run, (4) time series of Nino3 SST when the restoring SST is increased by 2 K, (5) time series of Nino3 SST when the restoring SST is lowed by 1 K. (From Clement et al. 1996)